

ÅBO AKADEMI UNIVERSITY  
FACULTY OF SCIENCE AND ENGINEERING

**Modifying nanocellulose hydrogels with *O*-acetyl-  
galactoglucomannan derivatives: tuning the surface  
hydrophilicity of the fiber surface**

Master's thesis

by

Pablo Vega

Carried out in the Laboratory of Wood and Paper Chemistry at

Åbo Akademi University

under the supervision of

PhD Xiaoju Wang and

Professor Stefan Willför

(22.05.2018)

## **Abstract**

### **Pablo Vega:**

Modifying nanocellulose hydrogels with *O*-acetyl-galactoglucomannan derivatives: tuning the surface hydrophilicity of the fiber surface

### **Master's thesis:**

Laboratory of Wood and Paper Chemistry, Faculty of Science and Engineering, Åbo Akademi University 2018, 67 pages, 21 figures, 4 tables

### **Supervisors:**

PhD Xiaoju Wang and Professor Stefan Willför, Laboratory of Wood and Paper Chemistry

### **Keywords**

Nanocellulose, cellulose nanofibrils, hemicelluloses, galactoglucomannans, polydimethylsiloxane, TEMPO-mediated oxidation, hydrogel, aerogel, surface hydrophilicity

Cellulose nanofibrils (CNFs) are emerging nanomaterials for such biomedical applications as cell culture platform and biomaterials in context of tissue engineering, thanks to their outstanding properties including bio-renewability, hydrophilicity, excellent mechanical strength and high surface area and aspect ratio originated from their nanodimensions.

This current master thesis work prepared CNF *via* 2,2,6,6-tetramethylpiperidine 1-oxyl radical (TEMPO) oxidation from a birch kraft pulp. The prepared CNF was elaborately characterised with material properties including the dry content, the surface charge density and the contents of reactive carboxylic acid groups and aldehyde groups introduced to the surface. A series of biopolymers of native galactoglucomannan (GGM) and its derivatives with polydimethylsiloxane were used to modify the CNF surface *via* the specific adsorption of the GGM block in the biopolymers to the cellulose surface. The adsorption of the GGM derivatives to the CNF was quantified by methanolysis in combination with gas chromatographic analysis.

Depending on the molecular structure in the GGM derivatives, these hemicellulose biopolymers rendered different wetting properties with adsorption onto the CNF membrane as characterised by contact angle measurements. Using a sequential solvent exchange process and freeze-drying method, aerogels were prepared out of all modified CNF membranes. Meanwhile, the adsorption of GGM derivatives onto CNF surface altered the fiber-fiber interactions to endow distinct topographical features compared with that in plain CNF aerogel.

## Acknowledgements

The work presented in this master's thesis has been carried out at the Laboratory of Wood and Paper Chemistry at Åbo Akademi University. Special acknowledgement goes to PhD Xiaoju Wang for helping and guiding me during the whole process and to Professor Stefan Willför and Docent Anna Sundberg for giving me the opportunity to use all the facilities and for giving me the opportunity of doing my master's thesis at Åbo Akademi.

I would like to thank all the staff in our laboratory, especially Weihua for his help and advices and also Jarl Hemming and Andrey Pranovich for all the help with instruments.

Finally, I would want to express my appreciation to my family, specially my father and my grandmother, for their support through these years of studying and life. Without your support this would have not been possible.

Turku, May 22<sup>th</sup>

Pablo Vega

## Table of contents

Abstract.....	2
Acknowledgements.....	4
Table of contents .....	5
List of abbreviations .....	7
List of figures.....	8
List of tables.....	9
1. Introduction .....	10
2. Review.....	12
2.1 Wood .....	12
2.2 Lignin.....	13
2.3 Hemicellulose.....	14
2.4 Cellulose.....	17
2.5 Nanocellulose.....	18
2.5.1 Cellulose nanofibrils .....	18
2.5.2 Cellulose nanocrystals .....	19
2.5.3 Bacterial nanocellulose.....	20
2.6 Hydrogels and aerogels .....	20
2.7 Nanocellulose preparation .....	23
2.7.1 Mechanical treatments .....	24
2.7.2 Pre-treatments .....	25
3. Materials and methods .....	29
3.1 Materials.....	29
3.2 Methods and determinations.....	30
3.2.1 Preparation of CNF via TEMPO oxidation .....	30
3.2.2 Determination of dry content.....	30
3.2.3 Determination of content of carboxylic acid and aldehyde groups..	31
3.2.4 Preparation of CNF hydrogels and aerogels.....	32

3.2.5 Quantification of GGMs adsorption by GC analysis .....	34
3.2.6 Fourier transform infrared spectroscopy.....	35
3.2.7 Contact angle measurement .....	35
3.2.8 Scanning electron microscope.....	35
3.2.9 Water uptake test on the aerogels .....	36
4. Results and discussion.....	37
4.1 Determination of the functional group content on the surface of CNF .....	37
4.2 Adsorption of GGM derivatives on CNF .....	40
4.3 Characterization of GGM-PDMS derivatives absorbed on CNF membranes.....	42
4.4 Surface wettability .....	45
4.5 Morphological features of the aerogels.....	47
4.6 Water uptake test of the aerogels.....	50
5. Summary.....	54
References .....	56

## List of abbreviations

<b>CA</b>	Contact angle
<b>CNC</b>	Celluloses nanocrystal
<b>CNF</b>	Cellulose nanofibrils
<b>EtOH</b>	Ethanol
<b>ECM</b>	Extracellular matrix
<b>FTIR</b>	Fourier transform infrared spectroscopy
<b>GC</b>	Gas chromatography
<b>GGMs</b>	Galactoglucomannans
<b>HDMS</b>	1,1,1,3,3,3-Hexamethyldisilazane
<b>PDMS</b>	Polydimethylsiloxane
<b>Q</b>	Water uptake ratio
<b>SEM</b>	Scanning Electron Microscopy
<b>TEMPO</b>	2,2,6,6-Tetramethylpiperidine-1-oxyl radical
<b>TCMS</b>	Trimethyl chlorosilane

## List of figures

<b>Figure 1.</b> Schematic structure of wood fibers (Dinwoodie et al., 1989) ....	13
<b>Figure 2.</b> Lignin distribution in lignocellulosic biomass (Doherty et al., 2011).....	14
<b>Figure 3.</b> Most important hemicelluloses in softwoods: a) xylan, b) glucomannan (Dutta et al., 2012).....	16
<b>Figure 4.</b> Illustration of the synthesis of the GGM-block-PDMS and GGM-PDMS-GGM triblock copolymer (Daniel Dax Doctoral Thesis, 2014) .....	16
<b>Figure 5.</b> Molecular structure of cellulose (Bajpai, 2017) .....	17
<b>Figure 6.</b> TEMPO oxidization of cellulose (Isogai & Kato, 1998).....	27
<b>Figure 7.</b> Enzymatic oxidation (Daniel Dax Doctoral Thesis, 2014) .....	28
<b>Figure 8.</b> A) GGM5; B) GGM5-PDMS-NH <sub>2</sub> ; C) GGM5-PDMS-GGM5.....	29
<b>Figure 9.</b> Plotted curve of the conductivity (Y axis) vs NaOH consumption (X axis).....	31
<b>Figure 10.</b> CNF.....	37
<b>Figure 11.</b> CNF (2).....	37
<b>Figure 12.</b> Relationships between the amount of NaClO added and either carboxylate and aldehyde contents or degree of polymerization of the oxidized groups (Isogai et al., 2011) .....	39
<b>Figure 13.</b> FTIR spectra for powder samples of GGM5, GGM5-PDMS-NH <sub>2</sub> , and GGM5-PDMS-GGM5.....	44
<b>Figure 14.</b> FTIR spectra of the membranes of CNF + GGM5, CNF + GGM5-PDMS-NH <sub>2</sub> and CNF + GGM5-PDMS-GGM5 .....	44
<b>Figure 15.</b> Contact angle measurement performed on different membranes at the first water drop contact .....	46
<b>Figure 16.</b> Dynamic contact angle measurements performed on different membranes within 20 s after the first contact with water drop .....	47
<b>Figure 17.</b> Top-view of an aerogel.....	48
<b>Figure 18.</b> Side-view of an aerogel .....	48
<b>Figure 19.</b> SEM images of the aerogels of different kinds.....	49
<b>Figure 20.</b> Aerogels placed in the cell for the swelling test.....	51
<b>Figure 21.</b> Water uptake ratio (mg/mg) of different aerogels vs immersion time (min) .....	53

## List of tables

<b>Table 1.</b> COOH groups before and after oxidation of CHO groups, with standard deviation.....	39
<b>Table 2.</b> Average contents of COOH and CHO groups in mmol/mg.....	40
<b>Table 3.</b> Adsorption of GGM derivates in CNF.....	42
<b>Table 4.</b> Average weights of the aerogels in mg.....	52

## **1. Introduction**

Over the last decades, the incredible demand of raw materials for industrial production has led to drastic environmental problems. Climate change, greenhouse gas emissions, water pollution, soil contamination, deforestation, and overexploitation of non-renewable resources have become major issues on our planet and present significant challenges for our society (Du et al., 2017). Therefore, society demands companies to be environmentally friendly and requires cleaner productions and green products, because environmental sustainability depends on industrial behaviour and utilization of natural resources (Sarmiento et al., 2005). In this scenario, bio-based materials have gained importance in replacement of the petroleum-based chemicals and materials (Zasadowski et al., 2014). The bio-based materials refer to the products whose main constituents are originally derived from living organisms (Razavi, 2018), which nowadays have been applied not only in traditional applications such as packaging and consumer goods but also in more value-added ones of electronics and pharmaceuticals.

Wood-derived biopolymers, including cellulose, hemicelluloses, and lignin can be obtained in high volume and purity via modern biorefinery approaches. Cellulose is the most abundant natural polymer on earth and it has been traditionally applied as textile and paper in our daily life. In the most recent decade, cellulose in nanoscale dimensions has been exploited as a new generation of nanomaterials in various disciplines.

Nanocelluloses have received renewed interests mainly due to their high specific surface area and aspect ratio resulted from the nano-sized dimension, as well as high stiffness of crystalline domains. Meanwhile, the abundant hydroxyl groups in the glucose unit provide sites for a broad spectrum of relevant chemical modifications to introduce functional groups as desired in specific applications. Given these outstanding material properties and derivation capabilities, nanocelluloses display a broad range of applicability as nanofillers in advanced composite materials, carrier of high surface area for catalysts, template for chiral nematic photonics, and so on. More specifically, cellulosic nanomaterials have shown great potential in such biomedical applications as cell culture platforms and soft tissue engineering constructs owing to their excellent

biocompatibility and the structural similarity between cellulose nanofibrils (CNFs) in hydrogel form and the extracellular matrix (ECM).

As exploited in recent years, wood-derived nanocellulose scaffolds in hydrogel form can be engineered to incorporate the cells and drugs and act as analogues to ECM found in soft tissues, that plays a pivotal role in determining the phenotype of cells (Bhattacharya et al., 2012). Hydrogels are important due to their structural and compositional similarities to ECM in terms of viscoelastic and diffusive transport characteristics. In hydrogels, a network of interconnected pores enables retention of high water content, and efficient transport of oxygen, nutrients and waste products. As a mimicking to ECM, tissue engineering scaffolds offer an artificial microenvironment to provide an appropriate surface and adequate spaces to foster and direct cellular attachment, migration, proliferation, and desired differentiation to specific cells in three dimensions, thus in the end to promote new tissue formation (Wan et al., 2011; Liu et al., 2016).

This master thesis work is focused on using a series of hemicellulose derivatives to modify the surface hydrophilicity of the CNF hydrogel via the biomimetic adsorption between hemicellulose and cellulose molecules. The aim is to investigate the correlation between the surface hydrophilicity of CNF hydrogel and the relevant cell attachment and proliferative behaviour.

## 2. Review

### 2.1 Wood

Wood is an organic material, mainly composed of cellulose and hemicelluloses built in a lignin matrix. It is commonly classified into two categories: hardwood (dicotyledons) and softwood (conifers). The wood fibers are made of cellulose (around 50%), hemicelluloses (around 25%) and lignin (around 25%). Lignin offers some protection to the wood from being degraded by common cellulolytic micro-organisms. There are two main forms: guaiacyl and syringyl lignin (Nilsson & Rowell, 2012). Wood cells give the tree the structural and physical properties, and are divided into primary and secondary layers, illustrated in Figure 1. The secondary layer is subdivided into  $S_1$ ,  $S_2$  and  $S_3$  layers. The  $S_2$  has the greatest influence in determining the properties of wood, because it occupies the largest volume of the cell wall (Rowell, 2012).

There are 5 different parts in the tree macro structure:

- Bark: Protects the tree from mechanical injuries and biological attacks
- Cambium: Located between bark and xylem (wood)
- Sapwood: Younger wood, living tissue. Water and nutrients are conducted from the roots to the leaves
- Heartwood: Due to chemical transformation and closing of pores this is the most resistant wood
- Pith: Is the central part

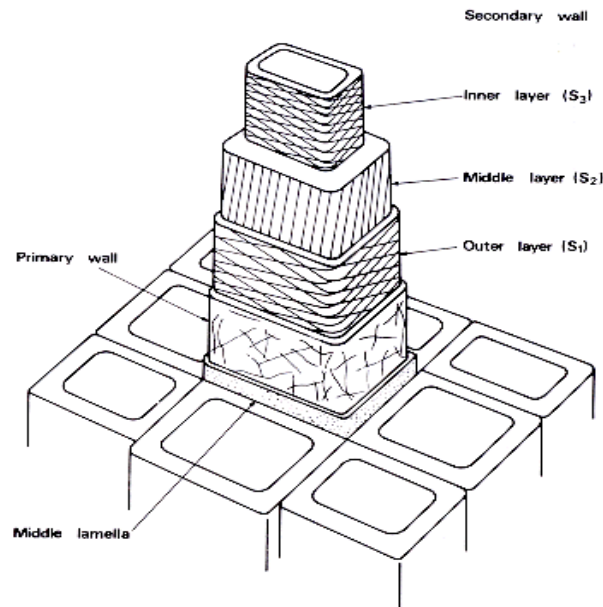


**Figure 1.** Schematic structure of wood fibers (Dinwoodie et al., 1989)

## **2.2 Lignin**

In nature, lignin presents a complex three-dimensional amorphous structure, arising from enzymatic dehydrogenative polymerization of three different cinnamyl alcohol monomers: sinapyl alcohol (syringyl (S) units), coniferyl alcohol (guaiacyl (G) units) and *p*-coumaryl alcohol (*p*-hydroxyphenyl (H) units) (Ralph et al., 2004; Mei et al., 2018).

Lignin accounts for approximately 30% of the organic carbon in the biosphere, and it is the second most abundant biopolymer of lignocellulosic biomass, after cellulose (Boerjan et al., 2003). It is commonly distributed in combination with hemicelluloses around the cellulose strands in primary and secondary cell walls, and it is covalently bonded to the carbohydrate/cellulose structure, as shown in Figure 2 (Doherty et al., 2011). Lignin acts primarily as a structural component, by adding strength and rigidity to the cell walls, but it also allows the transport of water and solutes through the vasculature system of the plants and provides physical barriers against invasions by phytopathogens, and other environmental stresses. It can also prevent the degradation of structural polysaccharides by its hydrolytic properties that influence cell wall degradability (Boerjan et al., 2003; Figueiredo et al., 2018).

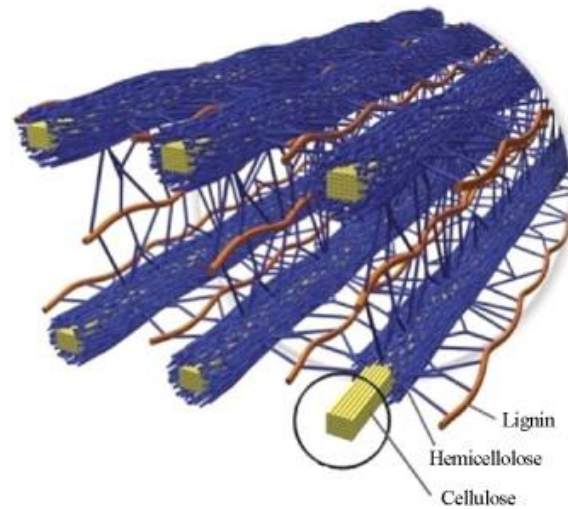


**Figure 2.** Lignin distribution in lignocellulosic biomass (Doherty et al., 2011)

## **2.3 Hemicellulose**

Hemicelluloses are soluble, branched and amorphous heteropolysaccharides, the majority of which are xylans in hardwoods and GGM's in softwood (Xu et al., 2018b). Hemicelluloses are present along cellulose in almost all plant cell walls. As well as cellulose, hemicellulose function as supporting material in the cell wall. After being fractionated from woody biomasses, the high physical affinity between hemicelluloses and cellulose surface is retained. This gives the hemicelluloses an applicable niche as anchor polymers to engineer the surface of cellulose fibers (Xu et al., 2018b). In contrast to cellulose, hemicelluloses:

- Are heteropolymers made up of monosaccharides such as pentoses, hexoses and uronic acids. The various types can vary widely with different plants and is sometimes used to classify the plant order (Mussatto & Teixeira, 2010)
- Might have a branched main chain. This amount of and types of branching varies depending on the source of the feedstock (Limayem & Rickie, 2012)
- Have a lower degree of polymerization (DP), between 100 to 400
- Are amorphous
- Might be soluble in water (Hendriks & Zeeman, 2009)

The main chain of hemicelluloses consists of either one sugar unit or two or more units. In hardwood, xylans are the major hemicellulose type, at around 80-90%. As an example, about 15-30% of the dry wood in birch is *O*-acetyl-4-*O*-methylglucuronoxylans. Pectins, rhamnoarabinogalactans and galactans are found in smaller amounts.

The water-soluble *O*-acetyl-galactoglucomannans are the main hemicellulose type in most softwood species, and they account for 10-20% of the wood material (Sjöström, 1993). As schematically illustrated in Figure 3, the GGM consists of a main chain of randomly distributed (1 → 4)-linked β-D-mannopyranosyl and (1 → 4)-linked β-D-glucopyranosyl units. (1 → 6)-linked α-galactopyranosyl and β-galactopyranosyl units occur as single-unit side chains attached to both the mannose and glucose units in the main chain (Willför et al., 2003; Xu et al., 2009). The degree of polymerization has been reported at between 100 and 150 and the molecular weights have been reported between 16000 and 24000 Da (Lundqvist et al., 2002). The water solubility of galactoglucomannans increases with increasing content and degree of branching of galactose (Capek et al., 2000; Ebringerová, 2005; Naidu et al., 2018).

Hydrophilic biopolymers may be altered hydrophobic by appropriate modifications either by physical treatment or chemical reactions applied to the surface (Cunha & Gandini, 2010).

In a previous doctoral thesis work by Dr. Daniel Dax (2014) performed in the Laboratory of Wood and Paper Chemistry, GGM was converted with a diamino polydimethylsiloxane (NH<sub>2</sub>-PDMS-NH<sub>2</sub>) in order to generate an amphiphilic GGM-block-structured derivative with a longer hydrophobic tail, as is shown in Figure 4. These GGM derivatives with PDMS in different block types is suitable for use as the anchor polymers to engineer the surface of cellulose fibers in terms of the surface hydrophilicity due to the instinct hydrophobicity of PDMS.

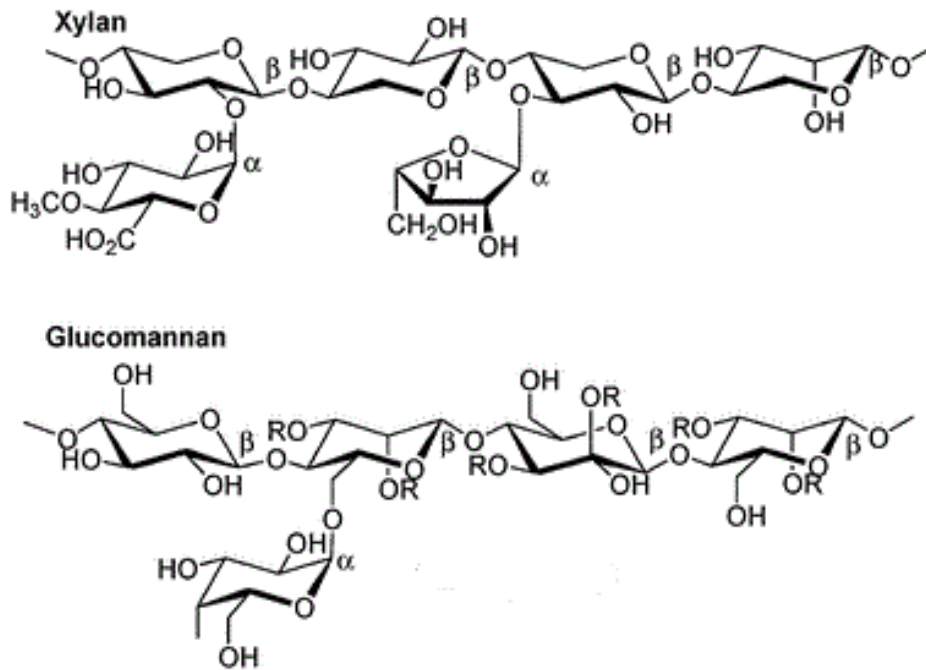


**Figure 3.** Most important hemicelluloses in softwoods: a) xylan, b) glucomannan (Dutta et al., 2012)

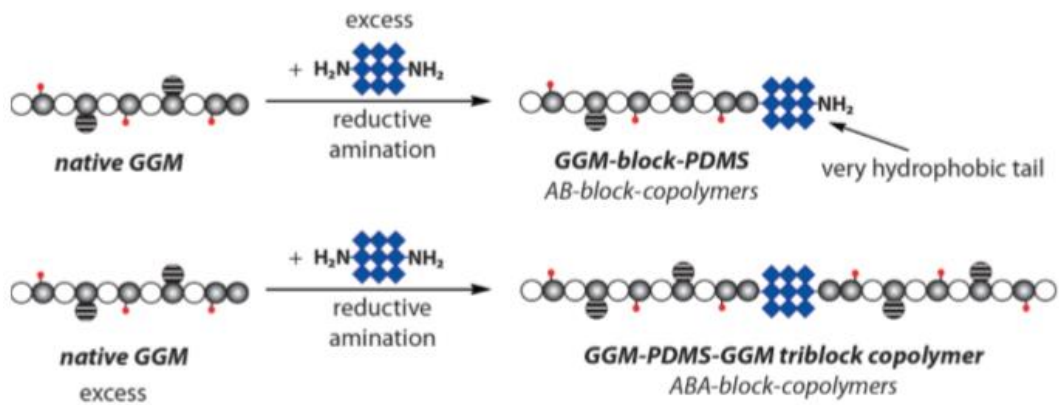


**Figure 4.** Illustration of the synthesis of the GGM-block-PDMS and GGM-PDMS-GGM triblock copolymer (Dax, 2014)



## **2.5 Nanocellulose**

Nanocelluloses are the cellulosic materials with defined dimensions on nanoscale, which can be derived from various cellulosic raw materials via chemical or physical treatments of different means (Klemm et al., 2011). With respect to the material morphology and the preparation means, nanocellulose can be derived into three types: cellulose nanofibrils (CNFs), cellulose nanocrystals (CNCs), and bacterial nanocellulose (BNC). Structure and properties of nanocellulose that are important include (Gardner et al., 2008; Lokanathan et al., 2017):

- Crystalline structure
- Morphology
- Surface properties
- Chemical and physical properties
- Properties in liquid suspension

Mechanical properties of nanocellulose are better than their lignocellulosic source biomass materials because of more uniform morphological structure. The average modulus of nanocellulose is 100 GPa, which is much higher than the base cellulosic materials (Dufresne, 2013).

### **2.5.1 Cellulose nanofibrils**

CNF, refers to the nanosized cellulose fibers, produced from wood fiber and plant fiber (Moon et al., 2011), that are disintegrated by exposing the pulp to high shear forces in a mechanical grinding of cellulose fibers. Cellulose microfibrils are biosynthesized by enzymes and they consist mainly of a crystalline cellulose core surrounded by hemicelluloses (Ramires & Dufresne, 2012). Chemical and enzymatic pretreatments can be done as well to help this fibers disintegration and to reduce the energy consumption. The nanofibrillated material consists of interconnected fibrils and microfibrils, whose width is 10-100 nm and length varies from 100 nm to several micrometers depending on the source of cellulose (Besbes et al., 2011).

The structure of CNF is not homogeneous and can consist in several components. Certain problems occur when trying to determine the fibril lengths due to difficulties to determine both ends.

### **2.5.2 Cellulose nanocrystals**

CNCs, also known as nanowhiskers, are rod-like cellulose nanomaterials of high crystallinity, which can be obtained from native fibers after acid hydrolysis to remove the amorphous regions. Commonly, strong mineral acids such as sulfuric acid, hydrochloric acid, phosphoric acid, and nitric acid are used (Seabra et al., 2018). Taking the method sustainability, as well as the economic aspects, into considerations, such organic acids as oxalic acid and maleic acid have been used to conduct the hydrolysis. Compared with CNF, CNC is intrinsically crystalline and rigid due to the solely retaining of the crystalline regions by removal of the amorphous regions in the native fiber structure via hydrolysis (Charreau et al., 2013; Salas et al., 2014). Depending on the source material and hydrolysis conditions (time and temperature), the dimensions of CNC vary a bit but with the diameter of 5-8 nm and length of 150 to 300 nm (Dash et al., 2012).

Presently, the research interests in CNCs in material science are raised upon their nanorod-like morphology and ultrastrong mechanical properties. The crystalline cellulose has a stiffness modulus in the order of 140-220 GPa, which is in the same magnitude as, for example, the synthetic Kevlar fibers, and is better than, for example, glass fibers. Both Kevlar fiber and glass fiber are being used commercially to reinforce plastics (Bajpai, 2017). Therefore, CNCs possess great potential as nanofiller materials. Owing to their nano-features, CNCs also have a high surface area as well as a low density of about  $1.6 \text{ g/cm}^3$ , which give strong applicable aspects of CNCs in constructing lightweight and advanced functional materials.

### **2.5.3 Bacterial nanocellulose**

BNC is an emerging cellulosic nanomaterial with unique properties produced by several species of bacteria, *Gluconacetobacter xylinus* being the most important one (Klemm et al., 2006; Gatenholm et al., 2010; Corral et al., 2017). It is also a green source for CNC preparation due to its environmentally friendly properties, such as renewability and cost-effective aspect, biocompatibility, biofunctionality and lack of toxicity (Jozala et al., 2016). This fine structure makes BNC different from other microbial polysaccharides, producing high water holding capacity, high tensile strength, high purity, and flexibility (Iguchi et al., 2000; Mondal, 2017). BNC has been used for a wide variety of applications such as textiles, cosmetics, food products, and medical applications. It may be used as a thickening, stabilizing, gelling, or suspending agent to produce a variety of low-calorie foods (Shi et al., 2014).

## **2.6 Hydrogels and aerogels**

The three classical phases of matter on Earth are solid, liquid, and gas, but the hydrogels are neither solid, liquid, nor gas. Like solids, hydrogels flow and like liquid, small molecules diffuse through a hydrogel but can have properties ranging from soft and weak to hard and tough (Paleos, 2012). The definition given by Dorothy Jordan in 1926 stated that “the colloidal condition, the gel, one which is easier to recognize than to define” (Lloyd, 1926). Researchers, over the years, have defined hydrogels in many different ways. Hydrogels, best described as fibrous networks of crosslinked polymers that contain large amounts of water, produced by the simple reaction of one or more monomers (Ahmed, 2015; Sathawong et al., 2018). Another definition is that it is a polymeric material that exhibits the ability to swell and retain a significant fraction of water within its structure, but will not dissolve in water (Thomas, 2012).

Hydrogels have received considerable attention in the past 50 years, due to their exceptional promise in wide range of applications (Buchholz & Graham, 1998). Hydrogels are currently viewed as water insoluble, crosslinked, three dimensional networks of polymer chains plus water that fills the voids between those chains (Wang, 2018). It is the crosslinking

that provides the structure (mechanical strength) and facilitates insolubility in water (Anseth et al., 1996; Del Valle et al., 2017). The ability of a hydrogel to hold significant amount of water implies that the polymer chain must have at least moderate hydrophilic character. By weight, hydrogels are mostly liquid.

There are different ways to classify hydrogels (Ahmed, 2015):

- Classification based on source

Hydrogels can be classified into two groups based on their natural or synthetic origins (Wen et al., 2013).

- Classification according to polymeric composition

The method of preparation leads to formations of some important classes of hydrogels. These can be exemplified by the following:

- Homopolymeric hydrogels are referred to polymer network derived from a single species of monomer, which is a basic structural unit comprising of any polymer network (Takashi et al., 2007). Homopolymers may have cross-linked skeletal structure depending on the nature of the monomer and polymerization technique.

- Copolymeric hydrogels are comprised of two or more different monomer species with at least one hydrophilic component, arranged in a random, block or alternating configuration along the chain of the polymer network (Yang et al., 2002).

- Multipolymer interpenetrating polymeric hydrogel (IPN), an important class of hydrogels, is made of two independent cross-linked synthetic and/or natural polymer component, contained in a network form. In semi-IPN hydrogel, one component is a cross-linked polymer and other component is a non-cross-linked polymer (Maolin et al., 2000).

- Classification based on configuration

The classification of hydrogels depends on their physical structure and chemical composition can be classified as follows:

- Amorphous (non-crystalline).

- Semicrystalline: A complex mixture of amorphous and crystalline phases.

- Crystalline.

- Classification based on type of cross-linking

Hydrogels can be divided into two categories based on the chemical or physical nature of the cross-link junctions. Chemically cross-linked networks have permanent junctions, while physical networks have transient junctions that arise from either polymer chain entanglements or physical interactions such as ionic interactions, hydrogen bonds, or hydrophobic interactions (Hacker & Mikos, 2011).

- Classification based on physical appearance

Hydrogels appearance as matrix, film, or microsphere depends on the technique of polymerization involved in the preparation process.

- Classification according to network electrical charge

Hydrogels may be categorized into four groups on the basis of presence or absence of electrical charge located on the cross-linked chains:

- Nonionic (neutral).

- Ionic (including anionic or cationic).

- Amphoteric electrolyte (ampholytic) containing both acidic and basic groups.

- Zwitterionic (polybetaines) containing both anionic and cationic groups in each structural repeating unit.

With the establishment of the first synthetic hydrogels by Wichterle and Lim in 1954 (Wichterle & Lim, 1960), the hydrogel technologies may be applied to hygienic products, drug delivery systems (Bajpai et al., 2008), sealing, artificial snow, agriculture, coal dewatering, food additives, pharmaceuticals, biomedical applications, tissue engineering (Khan et al., 2009) and regenerative medicines diagnostics, wound dressing, separation of biomolecules or cells and barrier materials to regulate biological adhesions, and biosensors (Krsko et al., 2009; Chang et al., 2011; Ahmed, 2015).

Aerogel is a colloidal material, derived from hydrogel, but in which the liquid component has been replaced by gas by performing freeze-drying. Essentially an aerogel is a dry, porous, but intact solid framework of a hydrogel of low-density (between 0.0011 to 0.5 g/cm<sup>3</sup>). Within the aerogel structure there is very little solid material, with up to 99.8% of the structure consisting of nothing but gas (De France et al., 2017). The majority of the aerogels are composed of silica, but carbon, iron oxide, organic polymers, semiconductor nanostructures, gold, and copper can also form aerogels. The aerogels possess favourable properties such as low mean free path diffusion, high specific surface area, low thermal conductivity, low sound speed and low refractive index and dielectric constant (Thomas, 2012).

As aerogel has such diverse chemical and physical properties, it is no surprise that it also has a wide range of applications. Aerogels have been used since the 1960's as the insulating material in spacesuits of NASA astronauts. NASA used it as well in the early 21st century to capture space dust aboard the Stardust spacecraft. Other applications:

- Chemical adsorber for cleaning up spills
- Thickening agents in paints and cosmetics
- As a drug delivery system owing to its biocompatibility
- In water purification
- Thermal insulation

## **2.7 Nanocellulose preparation**

Nanocellulose can be prepared from wood that was the first material utilized for the CNF production, and from all kind of lignocellulosic biomass. Renewable and biodegradable CNF reinforced composite materials are under extensive development and serve as a generation of sustainable and green materials in vast applications (Kalia et al., 2011). More importantly, cellulose nanomaterials add properties like high mechanical characteristics but in-low density (De Mesquita et al., 2010; Abdul Khalil et al., 2014).

CNF can be prepared by homogenization, using high pressure homogenizers as well as ultrasonic homogenizers, grinders and

microfluidizers (Jonoobi et al., 2015). The challenging aspect with the mechanical processes is the high energy consumption, since a large number of cycles are needed to defibrillate the fibers (Mishra et al., 2018). Therefore, the mechanical method can be further combined with certain pre-treatments to reduce the energy consumption (Zhang et al., 2012; Abdul Khalil et al., 2014). Those pre-treatments include TEMPO oxidation, enzymatic treatment (Lopez-Rubio et al., 2007), or alkaline acid pre-treatment (Alemdar & Sain, 2008).

### **2.7.1 Mechanical treatments**

#### **High pressure homogenization (HPH)**

This process includes passing the cellulose slurry at high pressure into a vessel through a very small nozzle. High speed and pressure as well as impact and shear forces decrease the size of fibers to nanoscale (Frone et al., 2011a; Xu et al., 2018a). HPH can be considered as an efficient method for refining of cellulosic fibers because of high its efficiency, simplicity and no need for organic solvents (Keeratiurai & Corredig, 2009; Lee et al., 2009). The clogging problem due to its very small orifice size can be overcome by reducing the fiber size before passing through HPH, therefore, mechanical pretreatments, like refining and grinding, are used before HPH (Abdul Khalil et al., 2014).

#### **Microfluidization**

Microfluidization functions like HPH, but includes intensifier pump to increase the pressure and interaction chamber to defibrillate the fibers using shear and impact forces against colliding streams and the channel walls (Ferrer et al., 2012). Several passes are necessary in order to reach a high degree of fibrillation. The morphological characterizations demonstrate that microfluidization can generate cellulose nanofibers with more homogenous size distribution than HPH (Abdul Khalil et al., 2014).

## **Grinding**

In the grinding equipment, there are two static and rotating grindstones and pulp slurry passes between these two stones. The mechanism of fibrillation in the grinder is to break down hydrogen bonds and cell wall structure by shear forces and individualization of nanoscale cellulose fibers (Siró & Plackett, 2010). Compared to the HPH process, less passes are required to obtain the defibrillation, but the crystallinity of cellulose nanofibers decreases with the increase of passing time (Abdul Khalil et al., 2014).

## **Cryocrushing**

Cryocrushing is another method for mechanical fibrillation of cellulose. In this process, water swollen cellulosic fibers are immersed in liquid nitrogen and subsequently crushed by mortar and pestle (Frone et al., 2011b). High impact forces are applied to the frozen cellulosic fibers leads to rupture of cell wall due to exert pressure by ice crystals and thus liberates the nanofibers (Siró & Plackett, 2010).

## **High intensity ultrasonication**

In this mechanical process, oscillating power is used to isolate cellulose fibrils by hydrodynamic forces of ultrasound (Cheng et al., 2009). During the process, cavitation leads to a powerful mechanical oscillating power and therefore, high intensive waves, which consists of formation, expansion and implosion of microscopic gas bubbles when molecules absorb ultrasonic energy (Chen et al., 2013).

All these methods involve high energy consumption, which can cause the decrease in both the yield and the fibril length. Researches are focused on finding environmentally friendly means of high efficiency and low cost to isolate nanocellulose (Abdul Khalil et al., 2014).

### **2.7.2 Pre-treatments**

Energy consumption is the main drawback of the production of nanofibers by mechanical isolation processes. However, less energy utilization leads

to less defibrillation of cellulosic fibers and lower production of nanofibers (Chinga-Carrasco, 2011). Therefore, chemical pre-treatments are performed before mechanical defibrillation to promote the accessibility of hydroxyl groups, to increase the inner surface, to alter crystallinity and to break cellulose hydrogen bonds and consequently, to boost the reactivity of the fibers (Abdul Khalil et al., 2014). The two main pretreatments are enzymatic and TEMPO-mediated oxidation (Missoum et al., 2013)

### **Enzymatic bio-treatment**

Enzymes of specific activity are used to modify or degrade lignin and hemicelluloses while maintaining the cellulose portion. On the other hand, enzymes can also help in restrictive hydrolysis of several elements or selective hydrolysis of specified units in the cellulosic fibers (Janardhnan & Sain, 2006).

Wood fibers contain several organic compounds and a single enzyme cannot degrade the fibers. Commonly, a set of cellulases are involved and are categorized (Henriksson et al., 2007):

- Cellobiohydrolases: A and B type cellulases, which attack specifically the crystalline regions in cellulose
- Endoglucanases: C and D type cellulases, which attack the disordered regions in cellulose

### **Alkaline acid treatment**

Alkaline acid pretreatment is used before mechanical isolation of CNF for solubilization of lignin, hemicelluloses and pectins (Alemdar & Sain, 2008). This pretreatment includes three steps (Bhatnagar & Sain, 2005):

- Soaking fibers in 12-17.5 wt% sodium hydroxides (NaOH) solution for 2 h in order to raise the surface area of cellulosic fibers, and to make it more susceptible to hydrolysis
- Hydrolysing the fibers with hydrochloric acid (HCL) solution for 1 M at 60-80 °C to solubilize the hemicelluloses
- Treating the fibers with 2 wt% NaOH solution for 2 h at 60-80 °C would disrupt the lignin structure, and would also degrade the linkages between carbohydrate and lignin

## TEMPO oxidation

2,2,6,6-Tetramethylpiperidine-1-oxyl (TEMPO) oxidation is a kind of pretreatments that facilitates the isolation of nanofibers by selectively introduces carboxyl (acidic) groups at the C6 of glucose unit (Iwamoto et al., 2011). Interestingly, TEMPO-oxidation does not affect the structural properties of the nanocelluloses (Habibi et al., 2006). The mechanism of TEMPO oxidization of cellulose is illustrated in Figure 6. The approach employs sodium hypochlorite (NaClO) as an oxidation reagent, with catalytic amount of TEMPO and sodium bromide (NaBr) (Saito et al., 2009). In this oxidation reaction, the nature of resultant materials was extremely dependent on the initial materials. When native cellulose is used, even under harsh conditions, the oxidation happens only at the surface, and it would become negatively charged, whereas using mercerized and regenerated cellulose, a water-soluble salt can be obtained as the oxidized product (Siró & Plackett, 2010; Abdul Khalil et al., 2014).

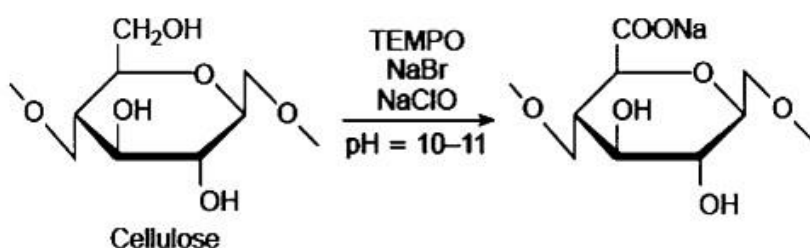


**Figure 6.** TEMPO oxidization of cellulose (Isogai & Kato, 1998)

Rheological properties of TEMPO-oxidized CNF have been studied (Lasseguette et al., 2008). The suspensions exhibited thixotropic and pseudo-plastic behaviour. Up to 0.23% as a critical concentration, viscosity of the suspension was proportional to the concentration. Below that level, the suspension was more Newtonian whereas it showed shear thinning behaviour above this concentration (Abdul Khalil et al., 2014).

Sequential periodate-chlorite oxidation was employed as an efficient and new pretreatment and was introduced to boost the nanofibrillation of hardwood through homogenization (Liimatainen et al., 2012). The oxidization process includes oxidizing hydroxyl groups to aldehyde groups

followed by oxidizing these aldehyde groups to carboxyl groups. In this system, sodium hypochlorite oxidizes TEMPO molecules into the corresponding *N*-oxoammonium ions, which then rapidly oxidize the primary hydroxyls to aldehydes. Sodium chlorite is used as the primary oxidant and this immediately oxidizes the formed aldehyde groups into carboxylic groups (Tanaka et al., 2012).

Some authors identify methods to avoid depolymerization during TEMPO reactions. For example, Shibata & Isogai (2003) observed that hydroxyl radicals formed from NaBrO and TEMPO at pH 10-11 can cause depolymerization during oxidation, and that some scavengers of reactive species could only partially suppress the depolymerization. Shinoda, Saito, Okita, and Isogai (2012) related the concentration of NaClO concentration with carboxylate content and the degree of polymerization (DP) of cellulose nanofibrils. The authors assumed that C6-aldehyde formed as an intermediate structure of TEMPO-oxidation could be associated with a  $\beta$ -elimination process, and that the elimination of such intermediates, due to post-oxidation or reduction of aldehydes formed, reduced such effect (Spier et al., 2017).

Enzymatic oxidation, shown in Figure 7, using galactose oxidase is even more selective than the TEMPO mediated oxidation and only specific sugar units can be targeted resulting in well-defined products (Parikka et al., 2009).

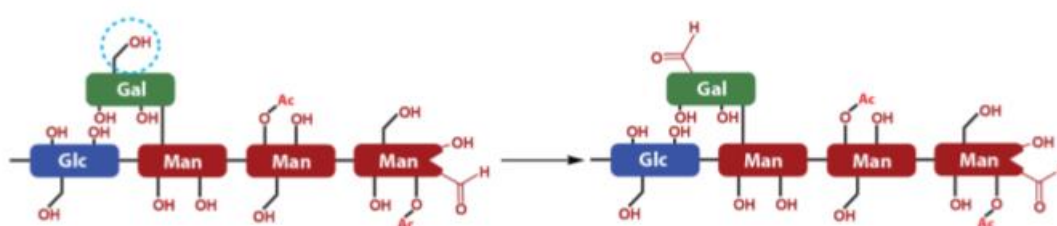


**Figure 7.**Enzymatic oxidation (Parikka et al., 2009)

### **3. Materials and methods**

#### **3.1 Materials**

Bleached birch kraft pulp (BKP), which was used in this work, is a predictably refined birch pulp that provides good strength, structure and surface properties. Bright and clean fibre structure helps to avoid any vessel picking problems that might be encountered.

Native GGM and two of its derivatives with PDMS were used in this work. The GGM fraction with a molar mass of 4.7 kDa is referred as GGM5 (I); AB type copolymer of GGM and PDMS with an average molar mass of 5.6 kDa is referred as GGM5-PDMS-NH<sub>2</sub> (II); ABA type copolymer of GGM and PDMS with an average molar mass of 10.3 kDa is referred as GGM5-PDMS-GGM5 (III). The molar mass of the diamino-terminated PDMS (NH<sub>2</sub>-PDMS-NH<sub>2</sub>) is 900 Da (Lozhechnikova et al., 2014). The native GGM and its derivatives are shown in Figure 8.

The other chemicals were used as received from commercial suppliers without further purification in the nanocellulose preparation and characterisation, which included TEMPO, NaBr, NaOH, NaClO, EtOH, HCl, NaCl, tert-butanol, acetic acid and NaClO<sub>2</sub>.

For the methanolysis and gas chromatography (GC) analysis, pyridine, carbohydrate calibration solution (0.1 mg/ml in MeOH), methanolysis reagent (waterfree 2 M HCl in MeOH), internal standard solution (0.1 mg/mL sorbitol and resorcinol in MeOH), hexamethyldisilazane (HDMS), trimethyl chlorosilane (TCMS) were also used as received from commercial suppliers without further purification.

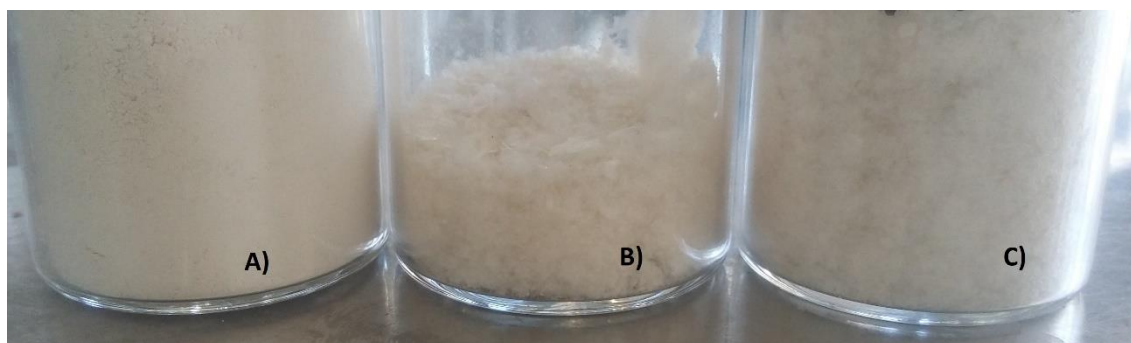


**Figure 8.** A) GGM5; B) GGM5-PDMS-NH<sub>2</sub>; C) GGM5-PDMS-GGM5

## **3.2 Methods and determinations**

### **3.2.1 Preparation of CNF via TEMPO oxidation**

The CNF hydrogel was prepared via TEMPO-mediated oxidation followed by mechanical defibrillation in a high-pressure homogenizer. In detail, 5 grams o.d. of bleached birch kraft pulp is mixed in 250 mL of distilled water using a domestic blender for a couple of minutes. The suspension was then stirred overnight at room temperature. 100 mL solution containing 32 mg of TEMPO (0.1 mmol/g fiber) and 200 mg of sodium bromide was mixed with the dispersed fiber suspension. The addition of 0.5 M NaOH was necessary to adjust the pH of the suspension to around 10.

The oxidation was initiated by adding the desired amount of 10% NaClO dropwise. 16.76 mL of NaClO was added within the one third of the designated reaction time while the pH should be maintained at 10.5 by the addition of 0.5 M NaOH. When no NaOH consumption was observed, the reaction was assumed to reach equilibrium. Typically, the total reaction time was around 5 hours.

The next step continued with washing of the TEMPO-oxidized cellulose. The oxidized cellulose was precipitated in ethanol with a ratio of 1:3 (v/v). In first cycle of centrifugation, the residual ethanol was removed. Then, the oxidized cellulose was intensively washed with deionized water in the other three cycles of centrifugation. The oxidized cellulose was defibrillated by a domestic blender during 2 min at high speed to obtain a hydrogel-gel like consistency of the CNF suspension. As the last step, the CNF hydrogel was subjected to mechanical homogenization with ATS-100 homogenizer in order to obtain more homogeneously defibrillation in the CNF hydrogel. Due to high shear forces as well as high speed and pressure, nanofibrils were obtained.

### **3.2.2 Determination of dry content**

Dry content determination was necessary to perform the following experiments. 3 samples of CNF were taken from the batch, weighed and set in 3 different aluminium covers, previously weighed. The samples were left in the oven at 107° C overnight and after 15 minutes cooling in a

desiccator, were weighed. Dry content of the 3 samples were obtained as well as the average dry content and standard deviation.

### 3.2.3 Determination of content of carboxylic acid and aldehyde groups

Conductometric titration was applied in order to determine the carboxylic acid group content. In detail, 50 mg o.d. of CNF were diluted to 0.1% (w/v) in water and 2 mL of 0.1 M HCl was added to exchange the sodium ions bound to the carboxyl groups by protons. In addition, 1 mL of 0.5 M NaCl was added to promote the dynamic distribution equilibrium of the ions and the slurry was sufficiently stirred for one and a half hour before titration. When a stable suspension was obtained, the mixture was titrated with 0.1 M NaOH at the rate of 0.1 mL/min as well as the conductivity and pH of the CNF suspension were registered during the titration. The carboxylic acid group content of the sample was then elaborated from a plotted curve of the conductivity vs consumption of NaOH. As is shown in Figure 9, results from the titration were plotted. From the 3 flat lines, 2 intersection points between the 3 flat lines gave 2 values on the X axis. The difference between these two values of consumption of NaOH was deemed to correspond with the content of COOH groups.

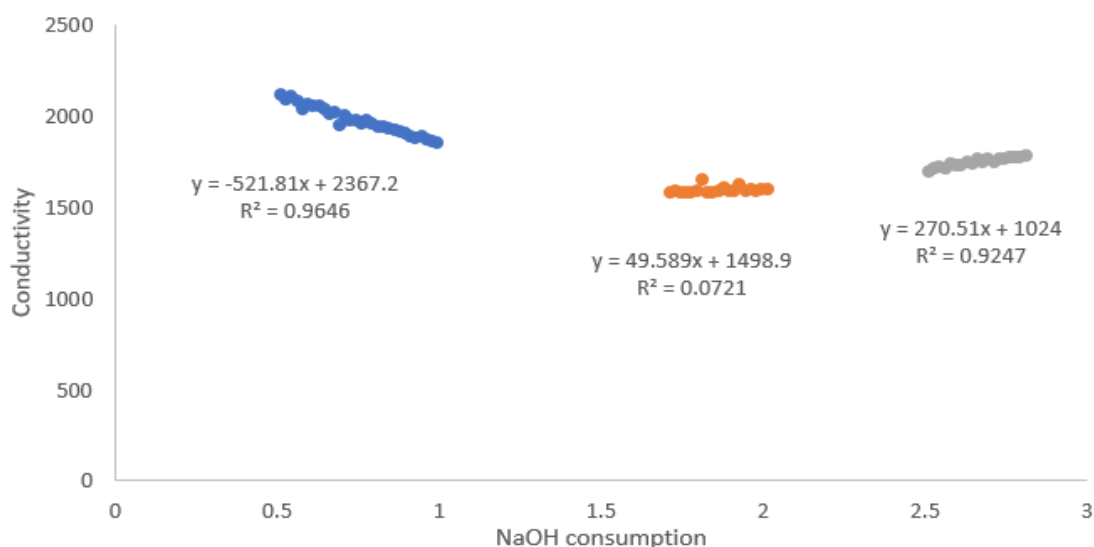


**Figure 9.** Plotted curve of the conductivity (Y axis) vs NaOH consumption (X axis)

The principle of conductometric titration is based on the fact that during the titration, one of the ions is replaced by the other and invariably these two ions differ in the ionic conductivity with the result that the conductivity of the solution varies during the course of the titration. The equivalence point may be located graphically by plotting the change in conductance as a function of the volume of titrant added. In order to reduce the influence of errors in the conductometric titration to a minimum, the angle between the two branches of the titration curve should be as small as possible. If the angle is very obtuse, a small error in the conductance data can cause a large deviation.

For the determination of the aldehyde group, further oxidation of the aldehyde groups on the fiber into carboxylic acid groups was performed. In detail, 0.28 gram of  $\text{NaClO}_2$  was added into a CNF solution, in which the amount of CNF in dry content corresponded to 250 mg, and the CNF solution was then diluted into 150 mL with distilled water. The pH of the suspension was kept between 4 and 5 with a 5 M aqueous acetic acid solution. The reaction run over 45 hours under stirring at room temperature. After that, the  $\text{NaClO}_2$  treated cellulose was washed thoroughly with distilled water by filtration. At last, a second titration was performed for the CNF suspension after the oxidation of aldehyde groups into carboxylic acid groups. The difference of carboxylic acid group content as determined in the first titration and in the second titration after oxidation are the content of aldehyde groups on the fiber surface of CNF, which are introduced in the TEMPO-mediated oxidation of cellulose.

#### **3.2.4 Preparation of CNF hydrogels and aerogels**

Four different types of hydrogels and aerogels were made in this work: i) CNF; ii) CNF modified by native GGM5, abbreviated as CNF+GGM5; iii) CNF modified by a GGM derivative with PDMS in AB block type, abbreviated as CNF + GGM5-PDMS-NH<sub>2</sub>; iv) CNF modified by a GGM derivative with PDMS but in ABA block type, abbreviated as CNF + GGM5-PDMS-GGM5. The first step to obtain the hydrogels, and after that the aerogels, is the creation of a membrane.

- CNF membrane: 300 mg o.d. of CNF was mixed into deionized water to make 0.1% suspension and stirred for half an hour. The CNF suspension

was filtered using a Millipore vacuum filtration system with a mixed cellulose ester membrane filter. The dense hydrogel of CNF formed on the top of the filter membrane was removed carefully, dried under a compression load of 5 kg iron specimen under ambient room temperature overnight and then further dried for 0.5 h in a vacuum desiccator at 40° C.

- CNF membrane with GGM5 adsorption: 300 mg o.d. of CNF was mixed and 30 mg GGM5 as dry powder were mixed into deionized water to make 0.1% suspension and stirred overnight. The CNF was then filtered using a Millipore vacuum filtration system with a mixed cellulose ester membrane filter. The dense hydrogel of CNF+GGM5 formed on the top of the filter membrane was removed carefully, dried overnight at ambient room temperature under a compression load of 5 kg iron specimen and further dried for 0.5 h in a vacuum desiccator at 40° C. The filtrate was collected to determine the GGM concentration by GC analysis.

- CNF membrane with GGM5-PDMS-NH<sub>2</sub> adsorption: 300 mg o.d. of CNF was mixed and 75 mg GGM5-PDMS-NH<sub>2</sub> as dry powder were mixed into deionized water to make 0.1% suspension and stirred overnight. The CNF was then filtered using a Millipore vacuum filtration system with a mixed cellulose ester membrane filter. The dense hydrogel of CNF+GGM5-PDMS-NH<sub>2</sub> formed on the top of the filter membrane was removed carefully, dried overnight at ambient room temperature under a compression load of 5 kg iron specimen and further dried for 0.5 h in a vacuum desiccator at 40° C. The filtrate was collected to determine the GGM5-PDMS-NH<sub>2</sub> concentration by GC analysis.

- CNF membrane with GGM5-PDMS-GGM5 adsorption: 300 mg o.d. of CNF was mixed and 138 mg GGM5-PDMS-GGM5 as dry powder were mixed into deionized water to make 0.1% suspension and stirred overnight. The CNF was then filtered using a Millipore vacuum filtration system with a mixed cellulose ester membrane filter. The dense hydrogel of CNF+ GGM5-PDMS-GGM5 formed on the top of the filter membrane was removed carefully, dried overnight at ambient room temperature under a compression load of 5 kg iron specimen and further dried for 0.5 h in a vacuum desiccator at 40° C. The filtrate was collected to determine the GGM5-PDMS-GGM5 concentration by GC analysis.

The dry membranes were cut into small circular pieces and left in water for 30 minutes, to swell. After this, water was removed and sequentially

replaced by 30% ethanol, 70% ethanol, 96% ethanol, absolute ethanol and tert-butanol at intervals of every 12 h. After the removal of tert-butanol, the hydrogels were kept in cell culture plates and then were left in liquid nitrogen for 30 minutes before freeze-drying. All solvent was sublimed during the freeze drying and the hydrogels were remained as intact aerogels.

### **3.2.5 Quantification of GGMs adsorption by GC analysis**

Acid methanolysis and GC-analysis were performed to quantify the amount of GGM and its derivatives adsorbed onto CNF (Sundberg et al., 1996). Accordingly, the procedures were performed as below:

First step is the methanolysis: Out of the solution obtained in the filtration, 4 samples of 2 g each one were taken and transferred to 4 different pear-shaped flasks with screw caps. In these 4 samples, the amount of GGM is unknown. In order to know the adsorption of GGM's in the membranes, a control solution is made. The amount of GGM's in this control solution is already known, in order to calculate the adsorption efficiency in the membranes. From this control solution, 4 samples of 2 g each one were taken and transferred to 4 different pear-shaped flasks. The 8 samples stayed overnight in the freezer and after that 48 hours in the freeze drier, with the screw caps open enough to let the vapour out.

Next step was the preparation of the 4 calibration samples. 1 mL of carbohydrate calibration solution (0.1 mg/mL in MeOH) were transferred to 4 different pear-shaped flasks and evaporate to dryness under nitrogen gas on a hot plate (50° C).

2 mL of methanolysis reagent (water free 2 M HCl in MeOH) were added to the 12 samples. All the samples were briefly shaken and treated in an ultrasonic bath for 1 minute. After this step, the 12 samples were kept in the oven for 3 hours.

In order to neutralize the excess of HCL, 200 µL of pyridine were added and the samples were mixed using a vortex mixer. 1 mL of internal standard (0.1 mg/mL sorbitol and resorcinol in MeOH) were added to all the samples; evaporation under nitrogen stream in a hot plate (50° C) was performed to remove the methanol. In order to remove all the methanol, samples were dried into a vacuum desiccator until nearly dry.

Silylation of the samples was the last step. 150  $\mu$ L of pyridine were added to the samples before shaking them. Time was needed to dissolve the samples. Addition of 150  $\mu$ L of HDMS and 70  $\mu$ L of TCMS were done to all samples before shaking them again. Ammonium chloride flocks were broken by placing the samples briefly in an ultrasonic bath. Samples were then shaken in the vortex mixer before the samples were left capped at room temperature overnight.

The silylated samples were transferred to GC autosampler vials by Pasteur pipettes, trying to avoid transferring any of the precipitate to prevent clogging the injection needle of the GC. Centrifugation of the vials was needed if there was problem to avoid the transferring of precipitates.

The GGM content in the solution collected from the CNF membrane filtration was analysed by acid methanolysis and GC analysis. As a control sample, a solution of only GGM or GGM-PDMS derivative with the same concentration as used in the CNF suspension in preparation of the corresponded membrane was analysed with the same protocol. The ratio of the integrated peak area for mannose in GC analysis between the filtration sample and the control sample was defined as the adsorption efficiency of GGM or GGM-PDMS derivatives onto the CNF surface.

### **3.2.6 Fourier transform infrared spectroscopy**

The Fourier Transform Infrared Spectroscopy (FTIR) measurements were performed with a Bruker Alpha series using the Alpha platinum ATR single reflection diamond ATR module. The samples were placed on the ATR plate and the results were evaluated using OPUS software from Bruker.

### **3.2.7 Contact angle measurement**

Water Contact Angle (CA) of the membranes were measured to determine their hydrophilicity. A 4  $\mu$ L water droplet was placed on the sample surface and the dynamic wetting of the surface was subsequently recorded using a high-speed camera on a CAM 200 contact angle goniometer (KSV Instrument Ltd., Finland) for a duration of 20 seconds. The contact angle values were obtained with OneAttension software.

### **3.2.8 Scanning electron microscope**

Scanning Electron Microscope (SEM) images of freeze-dried of CNF hydrogels were acquired using a Leo (Zeiss) 1530 Gemini Microscope.

Before imaging, the samples were sputter coated with gold for 2 min. The microscope was operating in secondary electron mode, and the images were acquired from a working distance of 7 mm, using 2.7 kV acceleration voltage.

### **3.2.9 Water uptake test on the aerogels**

The water uptake capacity was represented by the amount of water that can be absorbed into the aerogels. 12 aerogels were tested: 3 aerogels of CNF, 3 aerogels of CNF+GGM5, 3 aerogels of CNF+GGM5-PDMS-NH<sub>2</sub> and 3 aerogels of CNF+GGM5-PDMS-GGM5. The mass of each aerogel was weighed in prior to the tests. They were placed into wells in the culture plate and the deionized water was added. At immersion time of 5 min, 20 min, 1 h, 3 h, and 24 h the samples were then taken out gently, excessive water was carefully removed with tissue paper and the mass of each hydrogel with water uptake was weighed.

## **4. Results and discussion**

### **4.1 Determination of the functional group content on the surface of CNF**

Two batches of CNF with similar properties were made in this work. The dry content of the first CNF batch was 0.56% and in the second CNF batch it was 0.54%. After defibrillation in a high pressure homogenizer, the CNF showed a hydrogel-like consistency, as shown in Figure 10 and Figure 11.

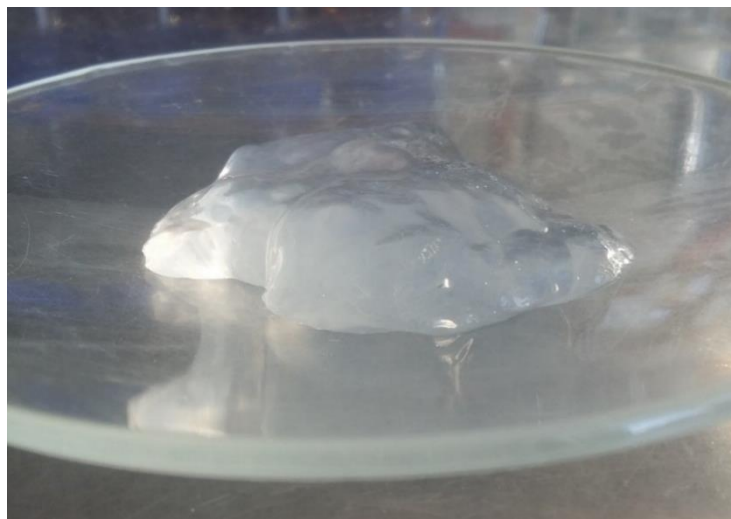


**Figure 10. CNF**



**Figure 11. CNF (2)**

As described in 2.7.2, carboxylic acid groups and aldehyde groups are introduced to the CNF surface during the TEMPO-mediated oxidation. The distribution ratio of carboxylic acid groups and aldehyde groups is greatly dependent on the dosage ratio of TEMPO and NaClO used in the reaction. The content of -COOHs on the CNF surface defines the surface charge density of the fibers, which strongly determines the fiber-fiber interaction and consequently the colloidal stability of the CNF hydrogel. A good dispersity of the TEMPO-oxidized CNF suspension requires a relatively high content of -COOH on the fiber surface to contribute the surface charge for stabilizing the fibers.

Meanwhile, it was indicated in the Jun Liu Ph.D Thesis (Liu, 2016), previously carried out at Laboratory of Wood and Paper Chemistry, that CNF hydrogel with an intermediate surface charge density supported the attachment and proliferation of fibroblasts in CNF hydrogel better than the one with an comparatively high surface charge density. Therefore, the CNF hydrogel was strategically prepared with an intermediate surface density throughout this thesis work. Thus, a comparatively low dosage of NaClO was employed in the TEMPO-mediated oxidation of pulp fibers.

When TEMPO is used in a low dosage but a large dosage of NaClO is employed in the reaction, a larger amount of carboxylic acid groups are on the surface (Masruchin et al., 2016). Figure 12 shows that the aldehyde groups formed on the cellulose fibers surfaces are susceptible to further oxidation by the TEMPO system, while those formed inside the cellulose fibers become relatively resistant to further oxidation probably by the formation of hemiacetal linkages with hydroxyl groups of cellulose sterically close to each other (Saito et al., 2006).

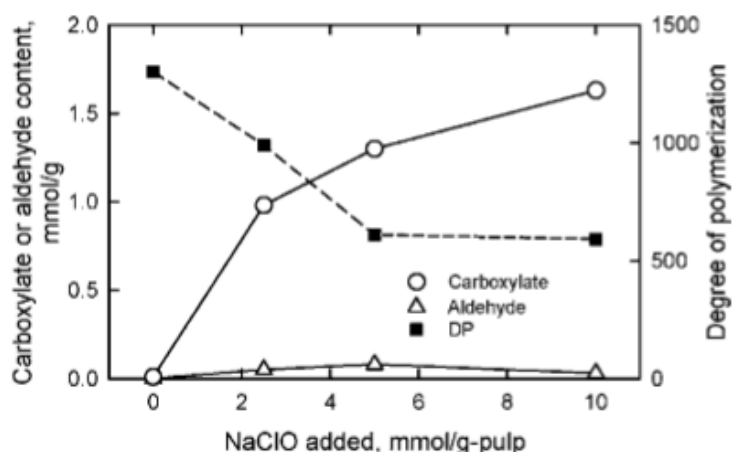


**Figure 12.** Relationships between the amount of NaClO added and either carboxylate and aldehyde contents or degree of polymerization of the oxidized groups (Isogai et al., 2011)

On another perspective, the functional group of -CHO also defines the chemical reactivity of the CNF materials and its quantitative information is an important parameter to consider in various applications of utilizing CNF.

Therefore, the protocol described in 3.2.2 was used to quantitatively measure the content of both the -COOH and the -CHO on the fiber surface. For the determination of the aldehyde groups, oxidation of those groups to carboxylic acid groups were performed. The difference between the COOH results before oxidation and results after oxidation are the amount of aldehyde groups. The content of -COOH and the -CHO groups on the CNF surface is given in mmol/mg as presented in Table 1.

**Table 1.** COOH groups before and after oxidation of CHO groups, with standard deviation

	Before oxidation	After oxidation
	COOH (mmol/mg)	COOH (mmol/mg)
Test 1	1.22	1.5
Test 2	1.26	1.6
Test 3	1.26	1.8
Standard deviation	0.02	0.15

**Table 2.** Average contents of COOH and CHO groups in mmol/mg

	Before oxidation	After oxidation	
	COOH (mmol/mg)	COOH (mmol/mg)	CHO (mmol/mg)
Average results	1.25	1.63	0.39

Comparing these results with previous studies, these values are among the average. It was indicated in the Master's Thesis by Mattias Strandberg, previously carried out at Laboratory of Wood and Paper Chemistry that the amount of carboxylic groups in CNF were 1.2 mmol/g for the unbleached CNF, 1.6 mmol/g for the self-bleached CNF and 1.8 mmol/g for the bleached CNF (Strandberg, 2017).

## **4.2 Adsorption of GGM derivatives on CNF**

GC is considered here as a dynamic method of separation of gas (or vapor) mixtures; the method is based on the movement of a mobile gas phase through a stationary phase and on different distribution of mixture components between mobile and stationary phases. In elution mode (which is more important for analytical purposes), the analysed sample is injected into the column and then is moved along the column by the carrier gas. In this mode, chromatogram (or elution curve) consists in a group of peaks. In ideal case every peak corresponds to single component of the sample (Kolomnikov et al., 2018).

By combining acid methanolysis and GC analysis, the adsorption amount of native GGM5 and its derivatives with PDMS was quantitatively determined. Table 3 presents the obtained results in several different expressions to indicate the quantity. The adsorption efficiency of GGM5 or its derivatives with PDMS onto the CNF surface, as listed in the third column, was calculated as the ratio of the integrated peak area for mannose in GC analysis between the filtration sample and the control sample. It tells how much of hemicellulose in weight percentage can be adsorbed onto the CNF surface. As stated in Section 3.2.3, the amount of CNF in each type of membranes is always 300 mg. Based on the adsorption efficiency, the quantity of the adsorbed GGM5 and its

derivatives with PDMS were calculated in unit of gram of hemicellulose per one gram of CNF, as displayed by column 4 in Table 3. Meanwhile, the corresponding units of GGM and PDMS in the adsorbed GGM5 or its derivatives were separately listed in column 5 and 6.

Unmodified GGM adsorbs on CNF due to the natural affinity of hemicelluloses toward cellulose (Eronen et al., 2011). Although hydrogen bonding usually is not the driving force for water adsorption, it does play a role during adsorption of polysaccharides on cellulose (Mohan et al., 2012). This inherent affinity is also likely to play a role in case of the GGM derivatives, due to the preserved structure of the GGM backbone. Owing to the similar structure, GGM can come in close contact with the cellulose and multiple hydrogen bonds are formed. As seen in Table 3, the adsorption efficiency of the GGM5-PDMS-NH<sub>2</sub> on CNF is higher compared with native GGM5. This indicates that the hydrophobicity of the PDMS block promotes the specific adsorption to some extent. As revealed in Daniel Dax Doctoral Thesis (Dax, 2014), this effect being stronger the higher the molar mass of the hydrophobic block. It is speculated that the hydrophobic interactions among the hydrophobic tails of PDMS has inhibited the desorption of GGM derivatives from the fiber surface. Although, in the case of GGM5-PDMS-GGM5, the adsorption efficiency was low in comparison with GGM5-PDMS-NH<sub>2</sub>. Still, because of the larger molecular weight of GGM5-PDMS-GGM5, more GGM units were actually adsorbed but less PDMS units were associated due to the block ratio of 2:1 in GGM5-PDMS-GGM5.

The solubility and adsorption of the GGM5-PDMS-NH<sub>2</sub> derivative on CNF might also be affected by the presence of the amine group in its structure, but since there is only one group in a big molecule, this influence is rather insignificant.

**Table 3.** Adsorption of GGM derivatives in CNF

	Mass of GGM's or its derivatives in the adsorption (mg)	Mole of GGM's and its derivatives in the adsorption ( $\mu$ mole)	Adsorption efficiency (%)	Adsorption on CNF (g/g)	GGM's in the adsorbed GGM's derivatives ( $\mu$ mole)	PDMS in the adsorbed GGM's derivatives ( $\mu$ mole)
GGM5	30	6.38	38.93	0.038	2.48	0
GGM5-PDMS-NH <sub>2</sub>	75	13.39	57.00	0.142	7.63	7.63
GGM5-PDMS-GGM5	138	13.39	34.16	0.157	9.15	4.57

#### **4.3 Characterization of GGM-PDMS derivatives absorbed on CNF membranes**

FTIR is used as a fast and accurate tool for detecting and analysing organic materials. Infrared spectrum is a method for identifying molecular structures based of the atom vibration and rotation. Atoms of organic molecules that form chemical bonds and functional groups are in a constant state of vibration. When a bundle of IR (infrared radiation) beam with a continuous wavelength passes through the sample, the light of a particular wavenumber is absorbed, which causes the absorbance spectrum (Hou et al., 2018).

In general, FTIR can be used to perform both qualitative and quantitative analysis for biomass application (Hames et al., 2003). The qualitative analysis includes the identification of known substances by comparing the sample spectra with the standard spectra. In addition, it can be used to identify the chemical structure of unknown substances. As to the quantitative analysis, there are several principles to ensure the accuracy of the result. First, the absorption band must be the characteristic absorption band of the material. Second, the absorption intensity must have a linear relationship with the concentration of the measured substance, which can be described as obeying the Lambert-Beer law (Sun

et al., 2011). Third, the band should possess a large absorption coefficient and as less as overlap by other absorption bands in case of interference.

FTIR spectra were recorded for the powders of GGM5 and its derivatives of GGM5-PDMS-NH<sub>2</sub>, and GGM5-PDMS-GGM5, as shown in Figure 13. The spectrum of GGM5 was recorded as a reference, the asymmetric CH<sub>3</sub> stretching in Si-CH<sub>3</sub> was assigned to the signal at 2960 cm<sup>-1</sup> (Cai et al., 2010); at 3350 cm<sup>-1</sup> the stretch of OH could be detected (Xu et al., 2013); the signal at 1412 cm<sup>-1</sup> was assigned to the CH<sub>3</sub> asymmetric bending (Özgenç et al., 2017). In the spectrums for GGM5-PDMS-NH<sub>2</sub> and GGM5-PDMS-GGM5, the CH<sub>3</sub> symmetric bending vibration (CH<sub>3</sub> deformation in Si-CH<sub>3</sub>) was found at 1258 cm<sup>-1</sup>. Furthermore, the Si-O-Si asymmetric stretching could be detected at 1021 cm<sup>-1</sup> (Cai et al., 2010). The signal at 867 cm<sup>-1</sup> was the CH<sub>3</sub> symmetric rocking and the latter peak, at 798 cm<sup>-1</sup>, was assigned to the Si-C asymmetric stretching in Si-CH<sub>3</sub>. The carbonyl group stretching signal at 1624 cm<sup>-1</sup> (Xu et al., 2013) was in the GGM5 spectrum as well as in the GGM5-PDMS-NH<sub>2</sub> and in the GGM5-PDMS-GGM5 arising from the acetyl group in GGM units (Sola et al., 2018).

Figure 14 displays the FITR spectrums for the CNF membranes with GGM or its derivatives adsorbed. As seen, the Si-C asymmetric stretching in Si-CH<sub>3</sub> at 798 cm<sup>-1</sup> was only observed in the spectrums of both CNF + GGM5-PDMS-NH<sub>2</sub> and CNF + GGM5-PDMS-GGM5 but not in the spectrum of CNF + GGM5. This indicated the presence of PDMS units in the membranes of both CNF + GGM5-PDMS-NH<sub>2</sub> and CNF + GGM5-PDMS-GGM5. Meanwhile, the adsorption at 798 cm<sup>-1</sup> was found to be larger in membrane of CNF + GGM5-PDMS-NH<sub>2</sub> than in membrane of CNF + GGM5-PDMS-GGM5, which most likely corresponded to the higher content of PDMS units adsorbed onto the membrane of CNF + GGM5-PDMS-NH<sub>2</sub> membrane CNF as quantified in the adsorption (as seen in column 5 of Table 3).

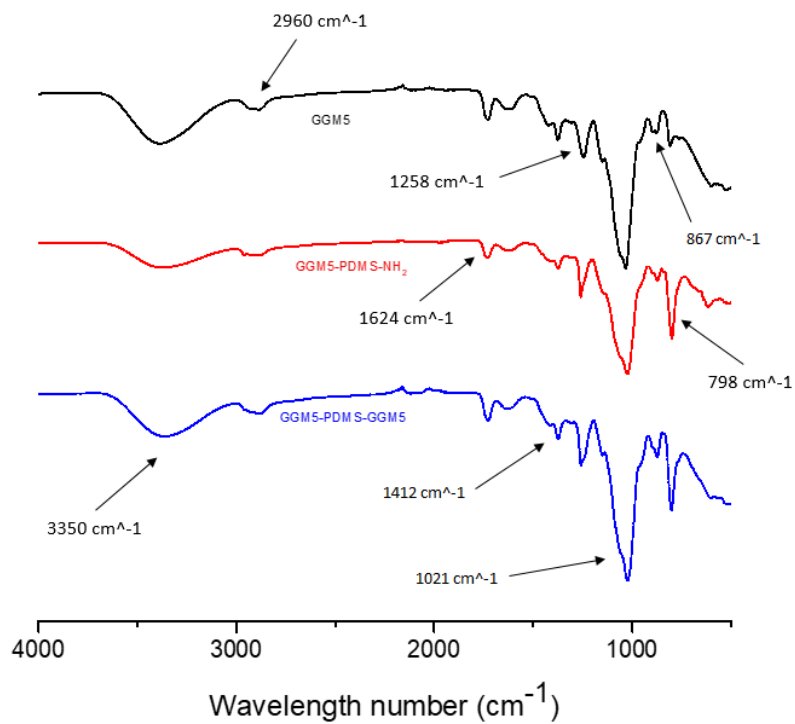


**Figure 13.** FTIR spectra for powder samples of GGM5, GGM5-PDMS-NH<sub>2</sub>, and GGM5-PDMS-GGM5

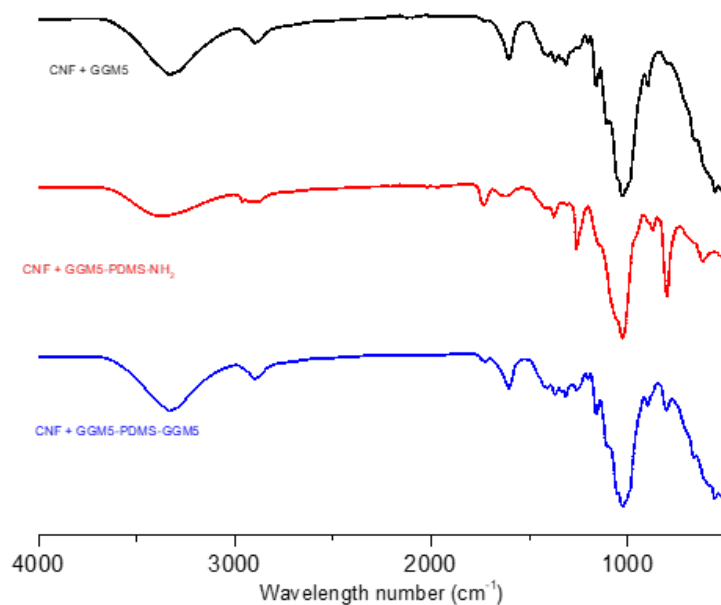


**Figure 14.** FTIR spectra of the membranes of CNF + GGM5, CNF + GGM5-PDMS-NH<sub>2</sub> and CNF + GGM5-PDMS-GGM5

#### **4.4 Surface wettability**

Inappropriate complement activation is often responsible for incompatibility reactions that occur when biomaterials are used (Engberg et al., 2015). Although considerable progress has been made in improving the properties of biomaterials, incompatibility reactions are still a problem (Ratner, 2007). The measurements of wettability represent essential scientific evaluation of properties for biomaterials. The most commonly used technique to quantify wettability of polymeric biomaterials surfaces are contact angle measurements (Agrawal et al., 2017).

In order to calculate the hydrophilicity of the membranes, contact angle measurements were done (Figure 15). The higher the contact angle is, the less hydrophilic the membrane is. The results show that the membrane containing GGM5-PDMS-NH<sub>2</sub> is the least hydrophilic, with a contact angle at a first drop contact of 73°, due to the presence of PDMS that is inherent hydrophobic. In the membrane containing GGM5-PDMS-GGM5, the presence of GGM5 in both ends compensate the presence of PDMS in the middle, but it was still less hydrophilic (69°) than the membrane containing only GGM5 (48°).

Previous studies demonstrate that the native PDMS surface usually shows the water contact angle of around 105°, and because this angle is higher than 90°, PDMS is considered to be hydrophobic (Kameya, 2017).

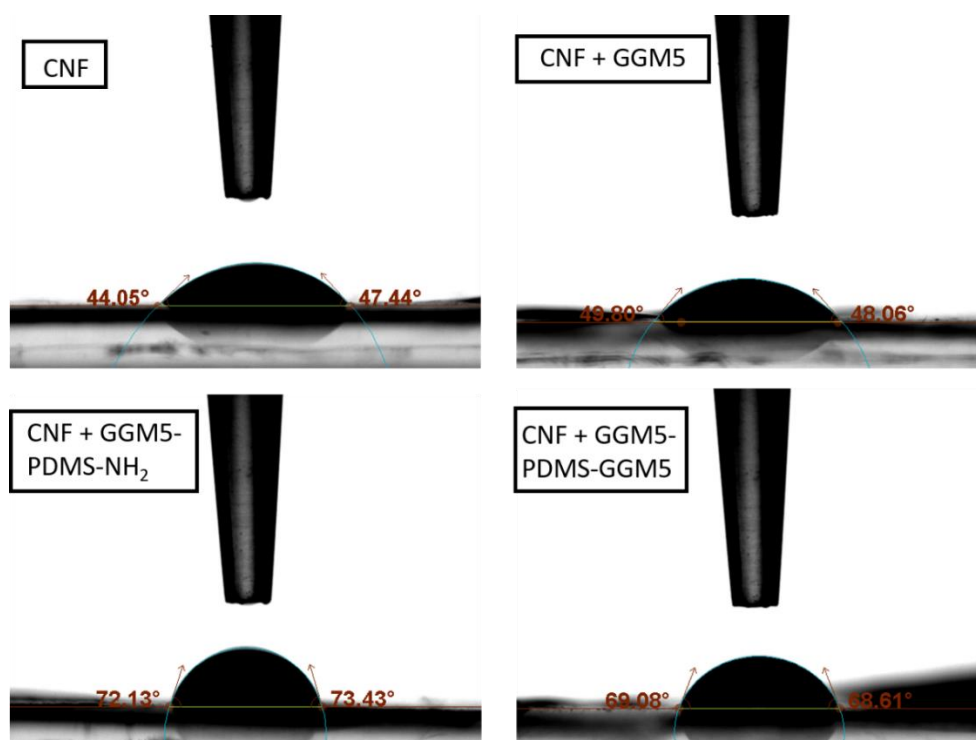


**Figure 15.** Contact angle measurement performed on different membranes at the first water drop contact

Figure 16 shows the results of the contact angle measurement for 20 seconds. In the samples c) and d) there are a peak at the beginning of the measurement (in the left side), peak that does not exist in the samples a) and b). The different GGM derivatives modify the CNF membranes surface but struggle to enhance hydrophobicity as long as the hydrophilic part of the GGM dominates the properties. However, using PDMS blocks, the presence of the highly hydrophobic tail with higher molecular mass improves the hydrophobicity of the CNF surface. Its shown in Figure 16c, where contact angle value for the GGM-PDMS block membrane is the highest one, that means that is the most hydrophobic. Therefore, the conclusion is that the natural hydrophilicity of the GGM chain, due to the presence of hydroxyl groups, is not being affected except by the presence of the PDMS tail that modifies the surface wettability and chemical functionality of the material.

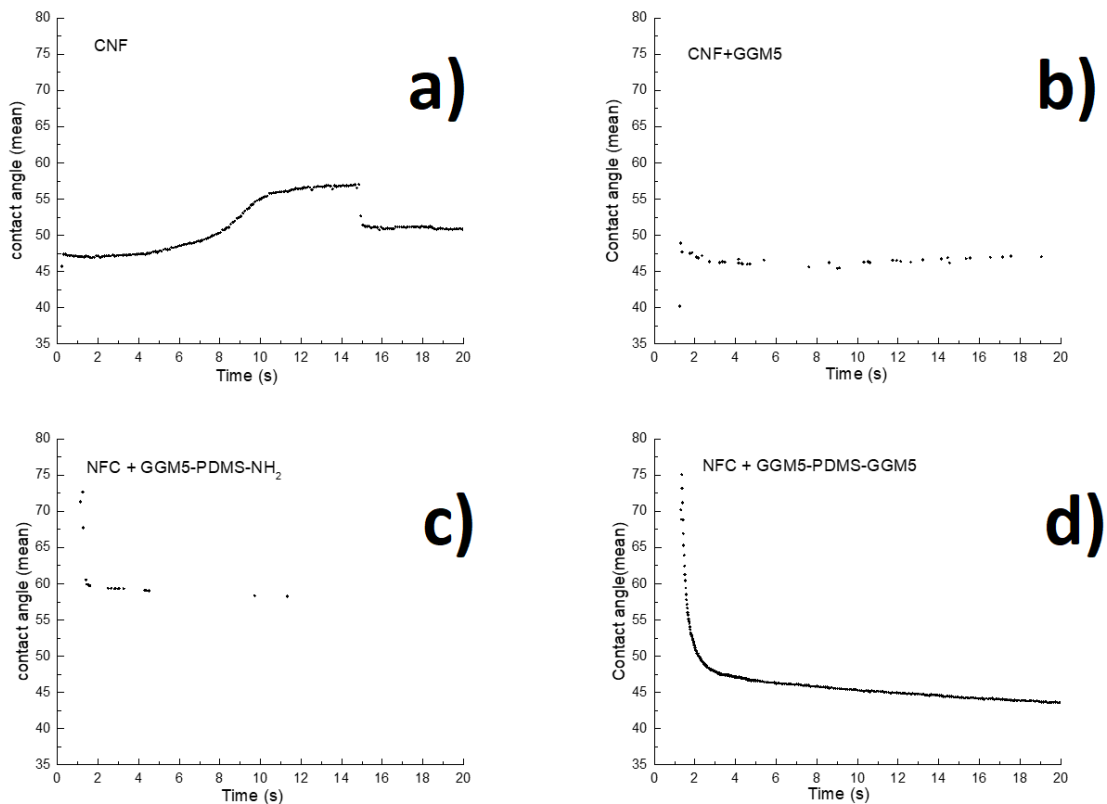


**Figure 16.** Dynamic contact angle measurements performed on different membranes within 20 s after the first contact with water drop

#### 4.5 Morphological features of the aerogels

The diameter of all the aerogels in this work is similar, around 5 mm, but the height is not the same due to the different components added, that result in different properties of the aerogels. The aerogels that have GGM5 (I) and GGM5-PDMS-GGM5 (III) are the ones that swelled the most due to the hydrophilicity properties of the GGM's, as its shown in the wettability test. The aerogels with GGM5-PDMS-NH<sub>2</sub> swelled less due to the presence of PDMS, which is ads hydrophobic properties to the surface.

After being treated in ethanol and tert-butanol, the aerogels have the same colour as the initial CNF. Is after been treated with nitrogen when the aerogels take the white colour showed in the Figure 17 and Figure 18.



**Figure 17.** Top-view of an aerogel

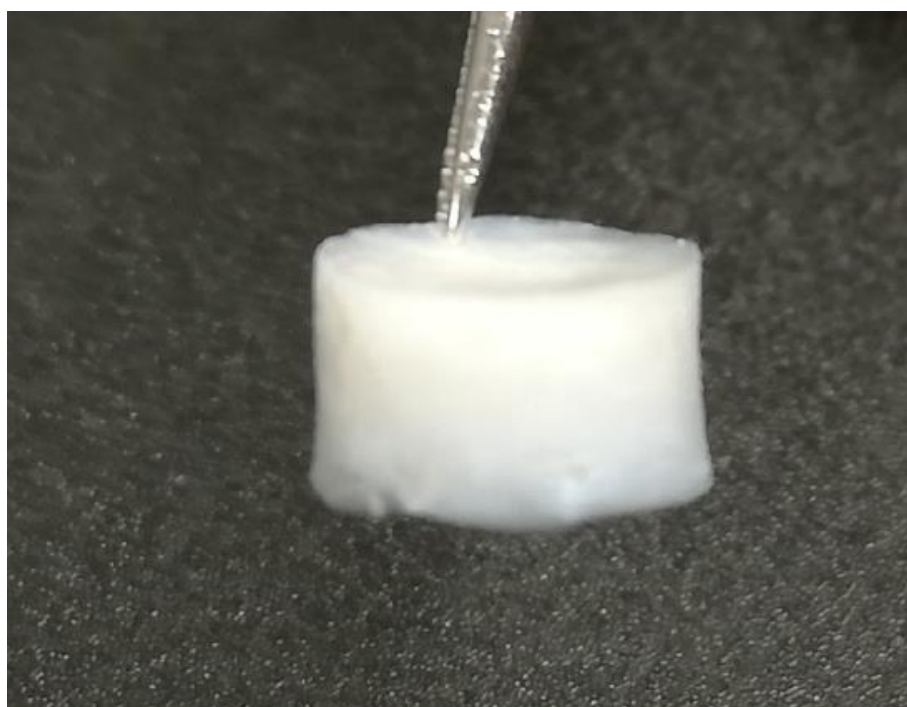


**Figure 18.** Side-view of an aerogel

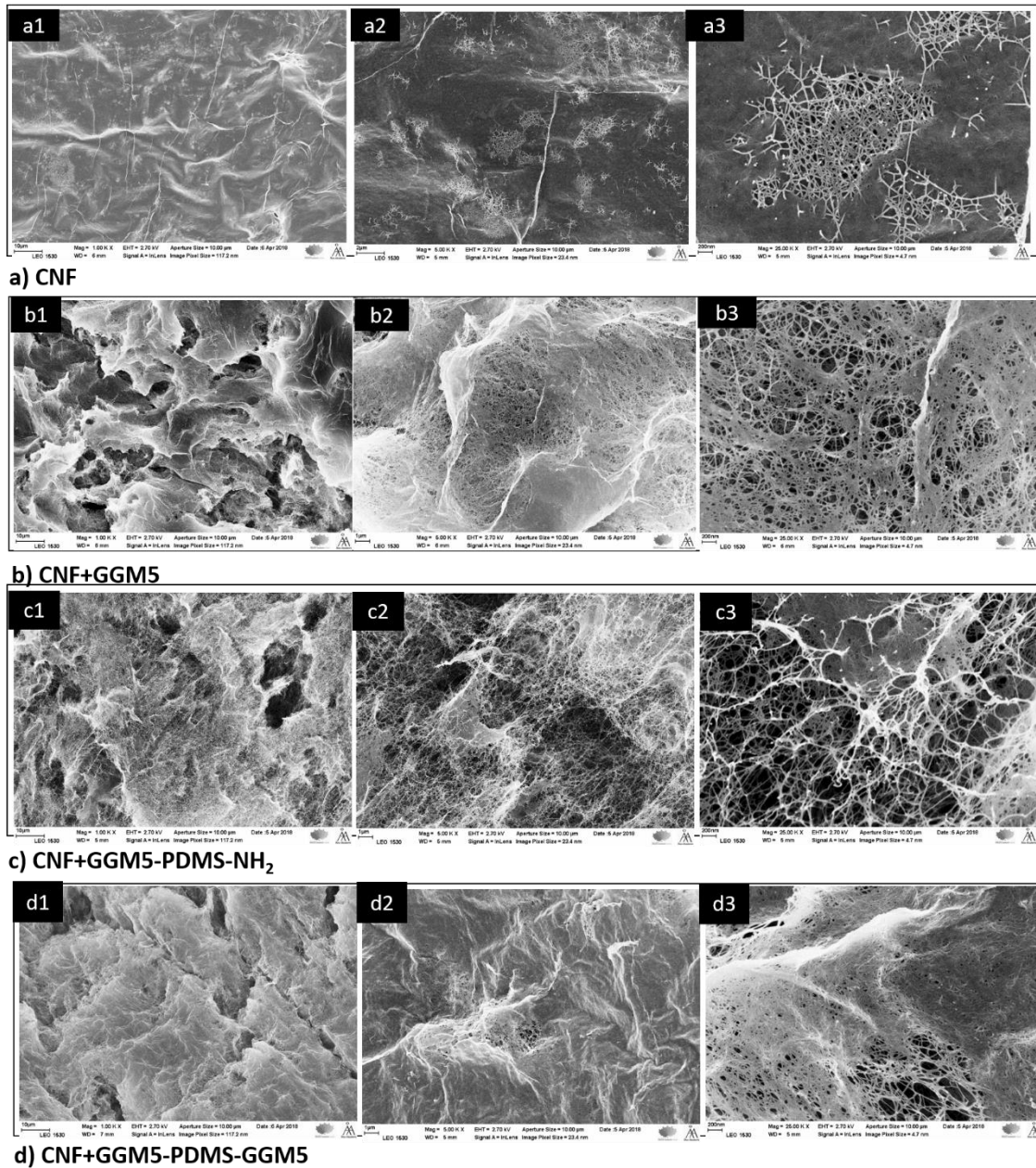


**Figure 19.** SEM images of the aerogels of different kinds

Figure 19 displays the SEM images (side-view) of the obtained aerogels from membranes of CNF, CNF + GGM5, CNF+GGM5-PDMS-NH<sub>2</sub> and CNF+GGM5-PDMS-GGM5, respectively in row a, b, c and d. Among these images, a1, b1 and c1 are in low magnification of  $\times 1K$ ; a2, b2 and c2 are in intermediate magnification of  $\times 5K$ ; and a3, b3 and c3 are in high magnification of  $\times 25K$ .

The CNF aerogel displayed a matt and compact appearance as the low magnification image displayed. In large magnification image, the network formed by entanglement of cellulose nanofibers was also found in some loosely packed areas. The adsorption of GGM5, GGM5-PDMS-NH<sub>2</sub>, and GGM5-PDMS-GGM5 onto the CNF altered the topographical features of the obtained CNF aerogels in different fashion. As shown in the image series of b1-b3, the aerogel of CNF + GGM5 showed a porous morphology and the entanglement of cellulose nanofibers in it were packed much looser compared to the aerogel of CNF. More interesting variation of the microstructure was found in the aerogel of CNF+GGM5-PDMS-NH<sub>2</sub> (as seen in image series of c1-c3). An entangled but open network of more individual cellulose nanofibers but less as bundles of cellulose fibers were spatially distributed through the entire imaged area. Even at the low magnification a 3D connected and fibrin-like network was visible and more fine structures was displayed in the image c3. However, the adsorption GGM5-PDMS-GGM5 on the CNF did not show similar modification as in the case of GGM5-PDMS-NH<sub>2</sub>. As observed in image series of d1-d3, compact packing of the cellulose fibers was resulted in the microstructure of aerogel of CNF+GGM5-PDMS-GGM5.

In correlation with the adsorption data in Table 3, it was speculated that adsorbed GGM5-PDMS-NH<sub>2</sub> on the CNF altered the fiber-fiber interactions due to the hydrophobic interactions among the PDMS tails, which probably caused the aggregates of PDMS tails and even to some extent directed the packing fashion of the nanofiber in the hydrogel formation. However, due to the ABA block type in GGM5-PDMS-GGM5, both heads of GGM5 were adsorbed onto CNF, which probably sterically hindered the hydrophobic interactions among the PDMS blocks in GGM5-PDMS-GGM5 molecules. Therefore, no similar type of modification to the surface morphology as in aerogel of CNF + GGM5-PDMS-NH<sub>2</sub> was seen in aerogel of CNF+GGM5-PDMS-GGM5.

#### **4.6 Water uptake test of the aerogels**

3 replicated samples of 4 different type of aerogels were employed in the swelling test. In total, 12 aerogels were placed in a cell culture plate as

shown in Figure 20. The CNF aerogels were placed in the column on the left side (A1 to C1). The aerogels of CNF+ GGM5 and CNF+GGM5-PDMS-NH<sub>2</sub> were respectively placed on the second (A2 to C2) and the third column (A3 to C3) as counted from the left side. The aerogels of CNF+GGM5-PDMS-GGM5 were placed on the right side (A4 to C4).

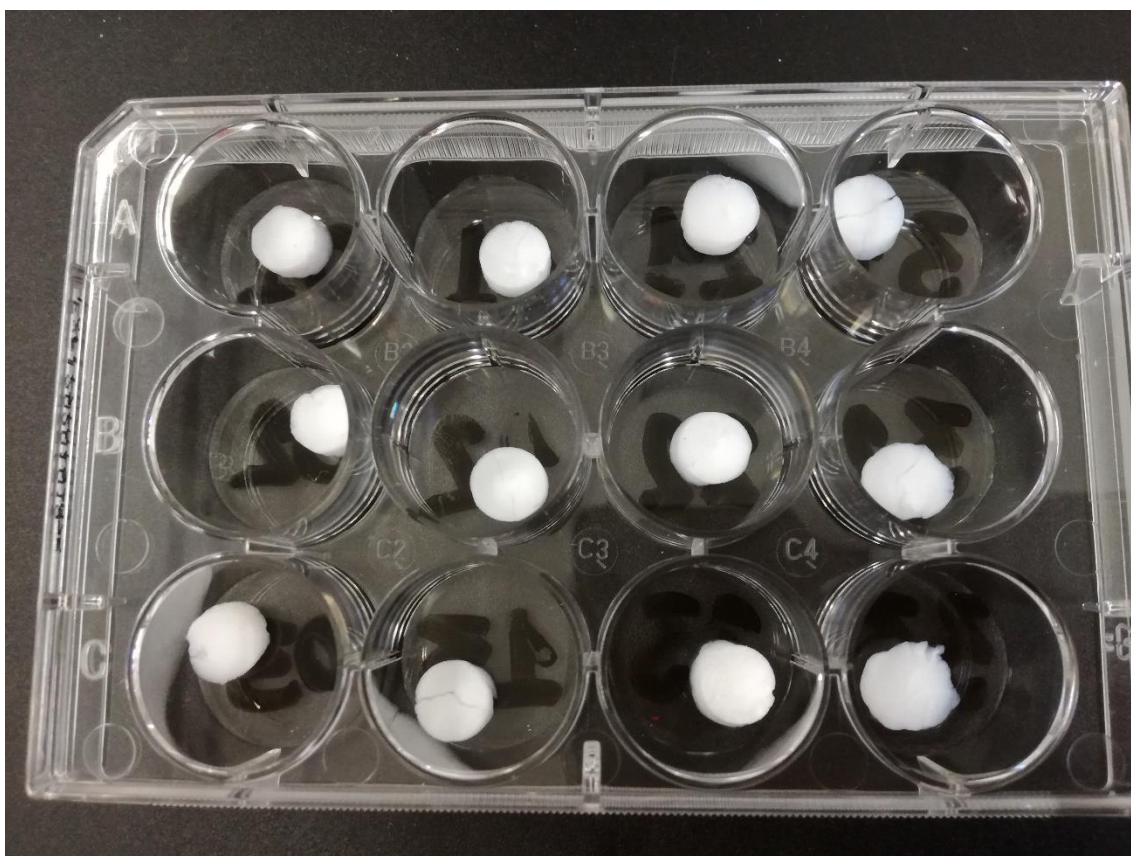


**Figure 20.** Aerogels placed in the cell for the swelling test

Table 4 shows the average weights of the hydrogels separated by composition. First measurement was taken when aerogels were dry and the other ones after deionized water was dropped (2<sup>nd</sup> one after 5 minutes in water; 3<sup>rd</sup> after 20 minutes; 4<sup>th</sup> after 1 hour; 5<sup>th</sup> after 3 hours and 6<sup>th</sup> after 24 hours).

**Table 4.** Average weights of the aerogels in mg

	Average mass					
	Dry	5 minutes	20 minutes	1 hour	3 hours	24 hours
CNF	2.6	214.1	245.1	267.5	300.1	327.1
CNF + GGM5	2.9	239.1	279.9	323.4	372.2	451.5
CNF + GGM5- PDMS-NH <sub>2</sub>	3.5	275.5	311.8	344.1	392.7	492.9
CNF + GGM5- PDMS-GGM5	4.43	412.2	443.4	482.2	635.9	757.0

The first weight value measured for the dry aerogel showed that all the hydrogels had different weights. In order to have a standardized expression of the water uptake capacity of the aerogel, the weight of water uptake in the hydrogel after swelling was divided by the weight value of the dry aerogel to give a water uptake ratio (Q)

$$Q = \frac{(m_t - m_0)}{m_0}$$

where  $m_t$  is the weight of the hydrogel at the time  $t$  and  $m_0$  is the initial weight of the corresponding dry aerogel.

Figure 21 presents the water uptake ratio of aerogels of different kinds vs the immersion time. The results clearly showed that all aerogels sorbed water by time with the same tendency. Overall, the aerogels of CNF+GGM5 and CNF+GGM5-PDMS-GGM5 demonstrated higher capability for sorbing water than the aerogels of CNF and CNF+GGM5-PDMS-NH<sub>2</sub>. This probably can be attributed to the GGM blocks adsorbed onto CNF promoted the capability of water uptake. In aerogel of CNF+GGM5-PDMS-NH<sub>2</sub>, PDMS blocks adsorbed is inherently hydrophobic and results smaller water uptake.

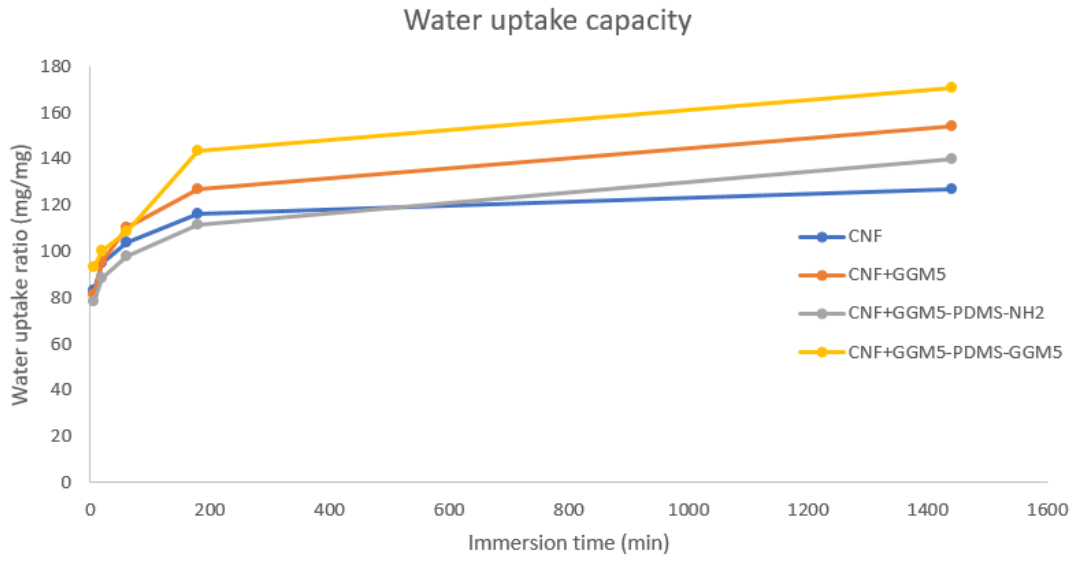


**Figure 21.** Water uptake ratio (mg/mg) of different aerogels vs immersion time (min)

## **5. Summary**

CNF is an emerging nanomaterial platform for such biomedical applications as cell culture platform and biomaterials in context of tissue engineering, thanks to its outstanding properties including bio-renewability, hydrophilicity, excellent mechanical strength and high surface area and aspect ratio originated from its nanodimensions.

The current master thesis work prepared CNF via TEMPO-mediated oxidation from a birch kraft pulp. The prepared CNF showed a hydrogel-like consistency after high pressure homogenization. With the reaction conditions employed during the TEMPO-oxidation, carboxylic acid groups of a density of 1.2 mmol/g as well as aldehyde groups of a density of 0.4 mmol/g were introduced to the CNF surface.

A series of biopolymer of native GGM and its derivatives with PDMS were used to modify the CNF surface via the specific adsorption of GGM block in the biopolymers to cellulose surface. The adsorption of these biopolymers to CNF was quantitatively determined by combining methanolysis and GC-analysis. The GGM5-PDMS-NH<sub>2</sub> demonstrated a higher adsorption efficiency to nanofiber surface in the preparation of CNF membrane. The presence of PDMS blocks in the membrane was further verified by FTIR measurements. Consequently, the modification of CNF surface by different GGM derivatives has rendered different wetting properties on the membrane surface. Above all, the adsorption of GGM5-PDMS-NH<sub>2</sub> on to CNF surface was able to tune the contact angle from 45° for the plain CNF membrane to 60° for the membrane of CNF + GGM5-PDMS-NH<sub>2</sub>.

Using a sequential solvent exchange process and freeze-drying method, aerogels were prepared out the CNF membranes. More interesting, the aerogel of CNF + GGM5-PDMS-NH<sub>2</sub> showed a fibrin-like and 3D spatially connected network of more individual cellulose nanofibers but less as bundles of cellulose fibers possible due to the hydrophobic interactions among the PDMS tails in the adsorbed molecules of GGM5-PDMS-NH<sub>2</sub>. The observed surface topological features might be of high interests for further tests in interactions with cells as a biomaterial.

In general, this series of GGM derivatives with PDMS has shown great potential to tune the surface hydrophilicity of CNF in a specific fashion,

which is highly correlated with the molecular structure in the block polymers. By modifying the CNF surface with the hemicellulose derivatives, the fiber-fiber interactions is also altered to endow distinct topographical features compare with that in plain CNF aerogel.

The work with the aerogels will continue outside this Master's Thesis with cell tests.

## References

- Abdul Khalil, H.P.S., Davoudpour, Y., Nazrul Islam, Md., Mustapha, A., Sudesh, K., Dungani, R. & Jawaid, M., 2014. Production and modification of nanofibrillated cellulose using various mechanical processes. *Carbohydrate Polymers*, 99(2), pp. 649-665.
- Agrawal, G., Negi, Y. S., Pradhan, S., Dash, M. & Samai, S. K., 2017. Wettability and contact angle of polymeric biomaterials. *Characterization of polymeric biomaterials*, pp. 57-81
- Ahmed, E.M., 2015. Hydrogel: Preparation, characterization and applications. *Journal of Advance Research*, 6(2), pp. 105-121
- Alemdar, A. & Sain, M., 2008. Biocomposites from wheat straw nanofibers: Morphology, thermal and mechanical properties. *Composite Science Technology*, 68, pp. 557-565
- Anseth, K. S., Bowman, C. N. & Branon-Peppas, L., 1996. Mechanical properties of hydrogels and their experimental determination. *Biomaterials*, 17(17), pp. 1647-1657
- Bajpai, A. K., Shukla, S. K., Bhanu, S. & Kankane, S., 2008. Responsive polymer in controlled drug delivery. *Progress in Polymer Science*, 33, p. 1088
- Bajpai, P., 2017. *Pulp and Paper Industry*. Amsterdam, Netherlands. Elsevier Inc.
- Besbes, I., et al., 2011. Nanofibrillated cellulose from TEMPO-oxidized eucalyptus fibers. Effect of the carboxyl content. *Carbohydrate Polymers*, 84(3), pp. 975-983
- Bhatnagar, A. & Sain, M., 2005. Processing of cellulose nanofiber reinforced composites. *Journal of Reinforced Plastic Composite*, 24, pp. 1259-1268
- Bhattacharya et al., 2012. Nanofibrillar cellulose hydrogel promotes three-dimensional liver cell culture. *Journal of Controlled Release*, 164(3), pp. 291-298
- Boerjan, W., Ralph, J & Baucher, M., 2003. Lignin biosynthesis. *Annual Review of Plant Biology*, 54, pp. 519-546

- Buchloz, F. L. & Graham, A. T., 1998. *Modern Superabsorbent Polymer Technology*. Wiley-VCH, New York, EEUU
- Cai, D., Neyer, A., Kuckuk, R. & Heise, H. M., 2010. Raman, mid-infrared, near-infrared and ultraviolet-visible spectroscopy of PDMS silicone rubber for characterization of polymer optical waveguide materials. *Journal of Molecular Structure*, 976(1-3), pp. 274-281
- Capek, P., Kubačková, M., Alföldi, J., Bilisics, L., Lišková, D. & Kákoniová, D., 2000. Galactoglucomannan from the secondary cell wall of *Picea abies* L. Karst. *Carbohydrate Resources*, 329(3), pp. 635-645
- Chang, C. & Zhang, L., 2011. Cellulose-based hydrogels: Present status and application prospects. *Carbohydrate Polymers*, 84(1), pp. 40-53
- Charreau, H., Foresti, M. L. & Vazquez, A., 2013. Nanocellulose patents trends: a comprehensive review on patents on cellulose nanocrystals, microfibrillated and bacterial cellulose. *Recent Pat Nanotechnology*, 7(1), PP. 56-80
- Chen, P., Yu, H., Liu, Y., Chen, X., Wang, X. & Ouyang, M., 2013. Concentrating effects on the isolation and dynamic rheological behaviour of cellulose nanofibers via ultrasonic processing. *Cellulose*, 20, pp. 149-157
- Cheng, Q., Wang, S. & Rials, T. G., 2009. Poly(vinyl alcohol) nanocomposites reinforced with cellulose fibrils isolated by high intensity ultrasonication. *Composites, Part A*, 40, pp. 218-224
- Chinga-Carrasco, G., 2011. Cellulose fibers, nanofibrils and microfibrils: The morphological sequence of MFC components from a plant physiology and fiber technology point of view. *Nanoscale Research Letters*, 6, p. 417
- Corral, M. L., Cerrutti, P., Vázquez, A. & Califano, A., 2017. Bacterial nanocellulose as a potential additive for wheat bread. *Food Hydrocolloids*, 67, pp. 189-196
- Cunha, A. G. & Gandini, A., 2010. Turning polysaccharides into hydrophobic materials: A critical review. Part 2. Hemicelluloses, chitin/chitosan, starch, pectin and alginates. *Cellulose*, 17(6), pp. 1045-1065

- Dash, R., Foston, M. & Ragauskas, A. J., 2013. Improving the mechanical and thermal properties of gelatin hydrogels cross-linked by cellulose nanowhiskers. *Carbohydrate Polymers*, 91(2), pp. 638-645
- Dax, D., 2014. Chemical Derivatization of Galactoglucomannan for Functional Materials, Doctoral Thesis. Laboratory of Wood and Paper Chemistry, Process Chemistry Centre, Department of Chemical Engineering, Åbo Akademi University
- De France, K. J, Hoare, T. & Cranston, E. D., 2017. Review of hydrogels and aerogels containing nanocellulose. *Chemistry of Materials*, 29(11), pp. 4609-4631
- De Mesquita, J. P., Donnici, C. L. & Pereira, F. V., 2010. Biobased nanocomposites from layer-by-layer assembly of cellulose nanowhiskers with chitosan. *Biomacromolecules*, 11, pp. 473-480
- Del Valle, L. J., Diaz, A. & Puggali, J., 2017. Review: Hydrogel for biomedical applications: Cellulose, Chitosan and Protein/Peptide Derivatives. *Gels*, 3(3), p. 27
- Dinwoodie, J. M., 1989. Wood: Nature's cellular polymeric fibre-composite. *The Institute of Metals*, p. 13
- Doherty, W. O. S., Mousavioun, P. & Fellows, C. M., 2011. Value-adding to cellulosic ethanol: Lignin polymers. *Industrial Crops and Products*, 33(2), pp. 259-276
- Du, X., Zhang, Z., Liu, W. & Deng, Y., 2017. Nanocellulose-based conductive materials and their emerging applications in energy devices- A review. *Nano energy*, 35, pp. 299-320
- Dufresne, A., 2013. Nanocellulose: A new ageless bionanomaterial. *Materials Today*, 16(6), pp. 220-227
- Dutta, S., De, S., Saha, B. & Imteyaz Alam, Md., 2012. Advances in conversion of hemicellulosic biomass to furfural and upgrading to biofuels. *Catalysis Science and Technology*, 2, pp. 2025-2036
- Ebringerová, A., 2005. Structural Diversity and Application Potential of Hemicelluloses. *Macromolecular Symposia*, 232(1), pp. 1-12

- Engberg et al., 2015. Prediction of inflammatory responses induced by biomaterials in contact with human blood using protein fingerprint from plasma. *Biomaterials*, 36, pp. 55-56
- Eronen, P., Österberg, M., Heikkinen, S., Tenkanen, M., Laine, J., 2011. Interactions of structurally different hemicelluloses with nanofibrillar cellulose. *Carbohydrate Polymers*, 86(3), PP. 1281-1290
- Ferrer, A., Filpponen, I., Rodriguez, A., Laine, J. & Rojas, O. J., 2012. Valorization of residual Empty Palm Fruit Bunch Fibers (EPFBF) by microfluidization: Production of nanofibrillated cellulose and EPFBFF nanopaper. *Bioresource Technology*, 125, pp. 249-255
- Figueiredo, P., Lintinen, K., Hirvonen, J. T., Kostianen, M. A. & Santos, H. A., 2018. Properties and chemical modifications of lignin: Towards lignin-based nanomaterials for biomedical applications. *Progress in Materials Science*, 93, pp. 233-269
- Frone, A. N., Panaitescu, D. M. & Donescu, D., 2011a. Some aspects concerning the isolation of cellulose micro- and nano- fibers. *U.P.B. Science Bulletin, Series B*, 73(2), pp. 133-152
- Frone, A. N., Panaitescu, D. M., Donescu, D., Spataru, C. I., Radovici, C. & Trusca, A., 2011b. Preparation and characterization of PVA composites with cellulose nanofibers, obtained by ultrasonication. *Bioresources*, 6(1), pp. 487-512
- Gardner, D. J., Oporto, G., Mills, R. & Samir, A., 2008. Adhesion and Surface Issues in Cellulose and Nanocellulose. *Journal of Adhesion Science and Technology*, 22(5-6), pp. 545-567
- Gatenholm, P. & Klemm, D., 2010. Bacterial nanocellulose as a renewable material for biomedical application. *Materials from renewable resources*, 35(3), pp. 208-213
- Habibi, Y., Chanzy, H. & Vignon, M. R., 2006. TEMPO-mediated surface oxidation of cellulose whiskers. *Cellulose*, 13(6), pp. 679-687
- Hacker, M. C. & Mikos, A. G., 2011. *Synthetic polymers, principles of regenerative medicine*, 2<sup>nd</sup> Ed, pp. 587-622

- Hames, B. R., Thomas, S. R., Sluiter, A. D., Roth, C. J. & Templeton, D. W., 2003. Rapid biomass analysis. *Applied Biochemistry and Biotechnology*, 105, pp. 5-16
- Hendriks, A. T. & Zeeman, G., 2009. Pretreatments to enhance the digestibility of lignocellulosic biomass. *Bioresources Technology*, 100(1), pp. 10-18
- Henriksson, M., Henriksson, G., Berglund, L. A. & Lindström, T., 2007. An environmentally friendly method for enzyme assisted preparation of microfibrillated cellulose (MFC) nanofibers. *European Polymer Journal*, 43, pp. 3434-3441
- Hou, X., Lv, S., Chen, Z. & Xiao, F., 2018. Applications of Fourier transform infrared spectroscopy technologies in asphalt materials. *Measurement*, 121, pp. 304-316
- Iguchi, M., Yamanaka, S. & Budhiono, A., 2000. Bacterial cellulose- a masterpiece of nature's arts. *Journal of Materials Science*, 35(2), pp. 261-270
- Isogai, A. & Kato, Y., 1998. Preparation of polyuronic acid from cellulose by TEMPO-mediated oxidation. *Cellulose*, 5, pp. 153-164
- Isogai, A., Saito, T. & Fukuzumi, H., 2011. TEMPO-oxidized cellulose nanofibers. *Nanoscale*, 3(1), pp. 71-85
- Iwamoto, S., Isogai, A. & Iwata, T., 2011. Structure and mechanical properties of wet-spun fibers made from natural cellulose nanofibers
- Janardhnan, S. & Sain, M., 2006. Isolation of cellulose microfibrils- An enzymatic approach. *Bioresources*, 1, pp. 176-188
- Jonoobi, M., Oladi, R., Davoudour, Y., Oksman, K., Dufresne, A., Hamzeh, Y. & Davoodi, R., 2015. Different preparation methods and properties of nanostructured cellulose from various natural resources and residues. *Cellulose*, 22(2), pp. 935-969
- Jozala, A., De Lencastre Novaes, L., Lopes, A., Ebinuma, V., Mazzola, P., Pessoa, A., Grotto, D., Gerenutti, M. & Marco, C., 2016. Bacterial nanocellulose production and application: a 10-year overview. *Applied Microbiology and Biotechnology*, 100(5), pp. 2063-2072

- Kalia, S., Dufresne, A., Cherian, B. M., Kaith, B. S., Auerousm, L., Njuguna, J., et al., 2011. Cellulose-based bio-and nanocomposites: A review. *International Journal of Polymer Science*
- Kameya, Y., 2017. Wettability modification of polydimethylsiloxane surface by fabricating micropillar and microhole arrays. *Materials Letters*, 196, p. 320-323
- Keeratiurai, M. & Corredig, M., 2009. Effect of dynamic high pressure homogenization on the aggregation state of soy protein. *Journal of Agricultural Food and Chemistry*, 57, pp 3556-3562
- Khan, F., Tare, R., Richard, O., Oreffo, R. & Bradley, M., 2009. Versatile biocompatible polymer hydrogels: scaffolds for cell growth. *Angewandte Chemical International Edition*, 48, p. 978
- Klemm, D. & Heublein, B., 2005. Cellulose: fascinating biopolymer and sustainable raw material. *Angewandte Chemie (International ed. In English)*, 44(22), pp. 3358-3393
- Klemm, D., Kramer, F., Moritz, S., Lindström, T., Ankerfors, M., Gray, D. & Dorris, A., 2011. Nanocelluloses: a new family of nature-based materials. *Biomacromolecules*, 50(24), pp. 5438-5466
- Klemm, D., Schumann, D., Kramer, F., Hebler, N., Hornung, M., Schmauder, H. & Marsch, S., 2006. Nanocelluloses as Innovative Polymers in Research and Application. *Advances in Polymer Science*, 205(1), pp. 49-96
- Kolomnikov, I. G., Efremov, A. M., Tikhomirova, T. I., Sorokina, N. M. & Zolotov, Y. A., 2018. Early stages in the history of gas chromatography. *Journal of Chromatography A*, 1537, pp. 109-117
- Krsko, P., Kaplan, J. B. & Libera, M., 2009. Spatially controlled bacterial adhesion using surface-patterned poly(ethylene glycol) hydrogels. *Acta Biomaterialia*, 5(2), pp. 589-596
- Lasseguette, E., Roux, D. & Nishiyama, Y. D., 2008. Rheological properties of microfibrillar suspension of TEMPO-oxidized pulp. *Cellulose*, 15, pp. 425-433
- Lee, S., Chun, S., Kang, I. & Park, J., 2009. Preparation of cellulose nanocellulose by high-pressure homogenizer and cellulose-based

composite films. *Journal of Industrial and Engineering Chemistry*, 15(1), pp. 50-55

Liimatainen, H., Visanko, M., Sirviö, J. A., Hormi, O. E. O. & Niinimäki, J. D., 2012. Enhancement of nanofibrillation of wood cellulose through sequential periodate-chlorite oxidation. *Biomacromolecules*, 13, pp. 1592-1597

Limayem, A. & Ricke, S.C., 2012. Lignocellulosic Biomass for Bioethanol Production: Current Perspectives, Potential Issues and Future Prospects. *Progress in Energy & Combustion Science*, 38, pp. 449-467

Liu, J., 2016. Wood-derived biomaterials for biomedical applications, Ph.D Thesis. Laboratory of Wood and Paper Chemistry, Process Chemistry Centre, Department of Chemical Engineering, Åbo Akademi University

Liu, J, Cheng, F., Grénham, H., Spoljaric, S., Seppälä, J., Eriksson, J. E., Willför, S. & Xu, C., 2016. Development of nanocellulose scaffolds with tuneable structures to support 3D cell culture. *Carbohydrate Polymers*, 148, pp. 259-271

Lloyd, D.J., 1926. In: Alexander, J. (ed.) Colloid Chemistry: Theoretical and Applied. *The Chemical Catalog Co*, 1, p. 7

Lokanathan, A. R., Kontturi, E., Linder, M. B., Rojas, O. J., Ikkala, O. & Gröschel, H., 2017. Nanocellulose-based materials in supramolecular chemistry. *Comprehensive Supramolecular Chemistry II*, pp. 351-364

Lopez-Rubio, A., Lagaron, J. M., Ankerfors, M., Lindström, T., Nordqvist, D., Mattozzi, A., et al., 2007. Enhanced film forming and film properties of amylopectin using micro-fibrillated cellulose. *Carbohydrate Polymer*, 68, pp. 718-727

Lozhechnikova, A., Dax, D., Vartiainen, J., Willför, S., Xu, C. & Österberg, M., 2014. Modification of nanofibrillated cellulose using amphiphilic block-structured galactoglucomannans. *Carbohydrate Polymers*, 110, pp. 163-172

Lundqvist, J., Teleman, A., Junel, L., Zacchi, G., Dahlman, O., Tjerneld, F. & Stålbrand, H., 2002. Isolation and characterization of galactoglucomannan from spruce. *Carbohydrate Polymers*, 48(1), pp. 29-39

- Maolin, Z., Jun, L., Min, Y. & Hongfei, H., 2000. The swelling behaviour of radiation prepared semi-interpenetrating polymer networks composed of polyNIPAAm and hydrophilic polymers. *Radiation Physics and Chemistry*, 58(4), pp. 397-400
- Masruchin, N., Park, B. & Causin, V., 2016. Characterization of cellulose nanofibrils-PNIPAAm composite hydrogels at different carboxyl contents. *Cellulose Chemical Technology*, 51(5-6), pp. 497-506
- Mei, Q., Shen, X., Liu, H. & Han, B., 2018. Selectively transform lignin into value-added chemicals. *Chinese Chemical Letters*
- Mishra, R. K., Sabu, A. & Tiwari, S. K., 2018. Materials chemistry and the futurist eco-friendly applications of nanocellulose: Status and prospect. *Journal of Saudi Chemical Society*
- Missoum, K., Belgacem, M. N. & Bras, J., 2013. Review: Nanofibrillated cellulose surface modification. *Materials*, 6(5), pp- 1745-1766
- Mohan, T., Spirk, S., Kargl, R., Doliska, A., Ehmann, H. M. A., Köstler, S., Ribitsch, V. & Stana-Kleinschek, K., 2012. Watching cellulose grow- Kinetic investigations on cellulose thin film formation at the gas-solid interface using a quartz crystal microbalance with dissipation (QCM-D). *Colloids and Surfaces*, 400, pp. 67-72
- Mondal, S., 2017. Preparation, properties and applications of nanocellulosic materials. *Carbohydrate Polymers*, 163, pp. 301-316
- Moon, R. J., Martini, A., Nairn, J., Simonsen, J. & Youngblood, J., 2011. Cellulose nanomaterials review: Structure, properties and nanocomposites. *Chem Soc Rev*, 40(7), pp. 3941-3994
- Mussatto, S. I. & Teixeira, J., 2010. Lignocellulose as raw material in fermentation process. *In Current Research, Technology and Education Topics in Applied Microbiology and Microbial Biotechnology*, pp. 897-907. FORMATEX
- Naidu, D. S., Hlangothi, S. P. & John, M. J., 2018. Bio-based products from xylan: A review. *Carbohydrate Polymers*, 179(1), pp. 28-41
- Nilsson, T. & Rowell, R., 2012. Historical wood-structure and properties. *Journal of Cultural Heritage*, 13(5), pp. s5-s9

Özgenç, Ö., Durmaz, S., Boyacı, I. H. & Eksi-Kocak, H., 2017- Determination of chemical changes in heat-treated wood using ATR-FTIR and FT Raman spectrometry. *Spectrochimica Acta Part A: Molecular and Biomolecular Spectroscopy*, 171, pp. 395-400

Paleos, G. A., 2012. What are hydrogels? *Pittsburgh Plastics Manufacturing*

Parikka, K., Leppänen, A. S., Pitkänen, L., Reunanen, M., Willför, S. & Tenkanen, M., 2009. Oxidation of Polysaccharides by Galactose Oxidase. *Journal of Agricultural and Food Chemistry*, 58(1), pp. 262-271

Ralph, J., Lundquist, K., Brunow, G., Lu, F., Kim, H., Schatz, P. F. & Marita, J. M., 2004. Lignins: Natural Polymers from oxidative coupling of 4-hydroxyphenyl-propanoids. *Phytochemistry Reviews*, 3(1-2), pp. 29-60

Ramires, E. C. & Dufresne, A., 2012. Cellulose nanoparticles as reinforcement in polymer nanocomposites. *Advances in Polymer Nanocomposites*, pp. 131-163

Ratner, B., 2007. The catastrophe revisited: blood compatibility in the 21st century. *Biomaterials*, 28, pp. 5144-5147

Razavi, M., 2018. Bio-based nanostructured materials. *Nanobiomaterials: Nanostructured materials for biomedical applications*, pp. 17-39

Rowell, R. M., 2012. *Handbook of Wood Chemistry and Wood Composites*. Boca Ratón, Florida. CRC Press

Salas, C., Nypelo, T., Rodriguez-Abreu, C., Orlando, C. & Rojas, O. J., 2014. Nanocellulose properties and applications in colloids and interfaces. *Current opinion in colloid and interface properties*, 19(5), pp. 383-396

Saito, T., Hirota, M., Tamura, N., Kimura, S., Fukuzumi, H., Heux, L et al., 2009. Individualization of nano-sized plant cellulose fibrils by direct Surface carboxylation using TEMPO catalyst Under neutral conditions. *Biomacromolecules*, 10, pp. 1992-1996

Saito, T. & Isogai, A., 2006. Introduction of aldehyde groups on surfaces of native cellulose fibers by TEMPO-mediated oxidation. *Colloids and Surfaces*, 289, PP. 219-225

Saito, T., Nishiyama, Y., Putaux, J.L., Vignon, M. & Isogai, A., 2006. Homogeneous suspensions of individualized microfibrils from TEMPO-

catalized oxidation of native cellulose. *Journal of the American Chemical Society*, 7(6), pp. 1687-1691

Sarmiento, M., Durao, D. & Duarte, M., 2005. Study of environmental sustainability: The case of the Portuguese polluting industries. *Energy*, 30(8), pp. 1247-1257

Sathawong, S., Sridach, W. & Techato K., 2018. Lignin: Isolation and preparing the lignin based hydrogel. *Journal of Environmental Chemical Engineering*

Seabra, A. B., Bernardes, J. S., Fávaro, W. J., Paula, A. J. & Durán, N., 2018. Cellulose nanocrystals as carriers in medicine and their toxicities: A review. *Carbohydrate Polymers*, 181(1), pp. 514-527

Shi, Z., Zhang, Y., Phillips, G. O. & Yang, G., 2014. Utilization of bacterial cellulose in food. *Food Hydrocolloids*, 35, pp. 539-545

Shibata, I. & Isogai, A., 2003. Depolymerization of cellouronic acid during TEMPO-mediated oxidation. *Cellulose*, 10(2), pp. 151-158

Shinoda, R., Saito, T., Okita, Y. & Isogai, A., 2012. Relationship between length and degree of polymerization of TEMPO-oxidized cellulose nanofibrils. *Biomacromolecules*, 13(3), pp. 842-849

Siró I. & Plackett, D., 2010. Microfibrillated cellulose and new nanocomposite materials: A review. *Cellulose*, 17, pp. 459-494

Sjöstrom, E., 1993. *Wood Chemistry*. Espoo, Finland. Elsevier Inc.

Sola, D., Lavieja, C., Orera, A. & Clemente, M. J., 2018. Direct laser interference patterning of ophthalmic polydimethylsiloxane polymers. *Optics and Lasers Engineering*, 106, pp. 139-146

Spier, V. C., Sierakowski, M. R., Reed, W. F. & Freitas, R. A., 2017. Polysaccharide depolymerization from TEMPO-catalysis: Effect of TEMPO concentration. *Carbohydrate Polymers*, 170, pp. 140-147

Strandberg, M., 2017. Preparation and properties of cellulose nanofibrils from pulps with different lignin content, Master's Thesis. Laboratory of Wood and Paper Chemistry, Process Chemistry Centre, Department of Chemical Engineering, Åbo Akademi University

- Sun, H., La, P., Yang, R., Zhu, Z., Liang, W., Yang, B., Li, A. & Deng, W., 2011. Innovative nanoporous carbons with ultrahigh uptakes for capture and reversible storage of CO<sub>2</sub> and volatile iodine. *Journal of Hazardous Materials*, 321, pp. 210-217
- Sundberg, A., Sundberg, K., Lillandt, C. & Holmbom, B., 1996. Determination of hemicelloses and pectins in wood and pulp fibres by acid methanolysis and gas chromatography. *Nord. Pulp Pap*, 11(4), pp. 216-219
- Takashi, L., Hatsumo, T., Makoto, M., Takashi, I., Takehiko, G. & Shuji, S., 2007. Synthesis of porous poly(*N*-isopropylacrylamide) gel beads by sedimentation polymerization and their morphology. *Journal of Applied Polymer Science*, 104(2), p. 842
- Tanaka, R., Siato, T. & Isogai, A., 2012. Cellulose nanofibrils prepared from softwood cellulose by TEMPO/NaClO/NaClO<sub>2</sub> systems in water at Ph 4.8 or 6.8. *International Journal of Biological Macromolecules*, 51(3), pp. 228-234
- Thomas, G. P., 2012. What is Aerogel? Theory, Properties and Applications. *Azom Materials*
- Wan, Y., Zuo, G., Yu, F., Huang, Y., Ren, K. & Luo, H., 2011. Preparation and mineralization of three-dimensional carbon nanofibers from bacterial cellulose as potential scaffolds for bone tissue engineering. *Surface and Coatings Technology*, 205(8-9), pp. 2938-2946
- Wang, Y., 2018. Programmable hydrogels. *Biomaterials*
- Wen, L., Xie, R., Ju, X., Wang, W., Chen, Q. & Chu, L., 2013. Nano-structured smart hydrogels with rapid response and high elasticity. *Nature Communications*, 4, article number 2226
- Wichterle, O. & Lim, D., 1960. Hydrophilic gels for biological use. *Nature*, 185, pp. 117
- Willför, S., Sjöholm, R., Laine, C., Roslund, M., Hemming, J. & Holmbom, B., 2003. Characterisation of water-soluble galactoglucomannans from Norway spruce wood and thermomechanical pulp. *Carbohydrate Polymers*, 52(2), pp. 175-187
- Xu, C., Willför, S., Holmlund, P. & Holmbom, B., 2009. Rheological properties of water-soluble spruce O-acetyl galactoglucomannans. *Carbohydrate Polymers*, 75(3), pp. 498-504

- Xu, F., Yu, J., Tesso, T., Dowell, F. & Wang, D., 2013. Qualitative and quantitative analysis of lignocellulosic biomass using infrared techniques: A mini-review. *Applied Energy*, 104, pp. 801-809
- Xu, J., Krietemeyer, E. F., Boddu, V. M., Liu, S. X. & Liu, W., 2018a. Productions and characterization of cellulose nanofibril from agricultural waste corn stover. *Carbohydrate Polymers*, 192, pp 202-207
- Xu, W., Wang, X., Sandler, N., Willför, S. & Xu, C., 2018b. Three-dimensional printing of wood-derived biopolymers: A review focused on biomedical applications. *ACS Sustainable Che Eng*
- Yang., L., Chu, J. S. & Fix, J. A., 2002. Colon-specific drug delivery: new approaches and in vitro/in vivo evaluation. *International Journal of Pharmacy*, 235, pp. 1-15
- Zasadowski, D., Yang, J., Edlung, H. & Norgren, M., 2014. Antisolvent precipitation of water-soluble hemicelluloses from TMP process water. *Carbohydrate Polymers*, 113(26), pp. 411-419
- Zhang, J., Song, H., Lin, L., Zhuang, J., Pang, C. & Liu, S., 2012. Microfibrillated cellulose from bamboo pulp and its properties. *Biomass and Bioenergy*, 39, pp. 78-83